Metabolic Toxicity Screening Using Electrochemiluminescence Arrays Coupled with Enzyme-DNA Biocolloid Reactors and Liquid Chromatography–Mass Spectrometry

Eli G. Hvastkovs,[1] John B. Schenkman,[2] and James F. Rusling[2,3]

[1]Department of Chemistry, East Carolina University, Greenville, North Carolina 27858; email: hvastkovse@ecu.edu

[2]Department of Cell Biology, University of Connecticut Health Center, Farmington, Connecticut 06269; email: jschenkm@neuron.uchc.edu

[3]Department of Chemistry, University of Connecticut, Storrs, Connecticut 06269; email: james.rusling@uconn.edu

Annu. Rev. Anal. Chem. 2012. 5:79–105

First published online as a Review in Advance on April 5, 2012

The *Annual Review of Analytical Chemistry* is online at anchem.annualreviews.org

This article's doi: 10.1146/annurev.anchem.111808.073659

1936-1327/12/0719-0079$20.00

Keywords

toxicity, genotoxicity, DNA damage, cytochrome P450, screening, high throughput, drugs, metabolism

Abstract

New chemicals or drugs must be guaranteed safe before they can be marketed. Despite widespread use of bioassay panels for toxicity prediction, products that are toxic to a subset of the population often are not identified until clinical trials. This article reviews new array methodologies based on enzyme/DNA films that form and identify DNA-reactive metabolites that are indicators of potentially genotoxic species. This molecularly based methodology is designed in a rapid screening array that utilizes electrochemiluminescence (ECL) to detect metabolite-DNA reactions, as well as biocolloid reactors that provide the DNA adducts and metabolites for liquid chromatography–mass spectrometry (LC-MS) analysis. ECL arrays provide rapid toxicity screening, and the biocolloid reactor LC-MS approach provides a valuable follow-up on structure, identification, and formation rates of DNA adducts for toxicity hits from the ECL array screening. Specific examples using this strategy are discussed. Integration of high-throughput versions of these toxicity-screening methods with existing drug toxicity bioassays should allow for better human toxicity prediction as well as more informed decision making regarding new chemical and drug candidates.

1. INTRODUCTION

Electrochemiluminescence (ECL): electrochemical generation of light using a luminescent species and a coreactant

Toxicity screening: refers to methods that can identify toxic compounds by in vitro tests, preferably in high throughput

Bioassays: assays that depend on cell cultures or animals

Biocolloid reactors: nanoparticles coated with enzymes and other reactive species; in this review, particles coated with DNA and enzymes

DNA adducts: products of the reaction of DNA, usually at bases, with other molecules

Analytical technologies have a rich history of helping to solve biomedical problems. For example, enzyme-based electrochemical biosensors provide methods of choice for diabetic patients to measure their blood glucose (1). Electrochemical biosensors have been developed to detect DNA for genetic analysis and protein biomarkers for disease detection (2, 3). Electrochemiluminescence (ECL), a type of electrochemically generated luminescence, has facilitated the sensitive detection of nucleic acids and proteins (4, 5). Liquid chromatography–mass spectrometry (LC-MS) has become an essential tool for a wide range of biomedical research (6–8). LC-MS also provides sensitive methodology for detecting DNA base adducts that are toxicity biomarkers (9, 10). Roughly a decade ago, our research team at the University of Connecticut combined nanoscience with some of the above techniques to yield molecularly based methods for new chemical and drug toxicity screening. This review relates the story of our methods-development journey.

First, we discuss the need for toxicity screening and the metabolic basis of toxic effects. Second, we briefly summarize alternative toxicity-screening bioassays to show how our methodology differs from and complements traditional and emerging methods. Third, we discuss the background of electrochemical DNA-damage and toxicity screening to place our methodology in context. Fourth, we discuss ECL array development and enzyme-DNA biocolloid reactor arrays as sample generators for LC-MS. Fifth, we describe a case study that combines both of these methods for toxicity assessment. Finally, we close with some predictions for the future of this research.

2. SCREENING FOR METABOLIC TOXICITY

New chemicals such as drugs and chemical products that can find their way into our bodies must be guaranteed safe before they can be marketed. For drugs, this assessment is carried out by first using panels of bioassays designed for this purpose, then progressing with animal toxicity studies, and finally, using human clinical trials. A wide range of bioassays for human toxicity prediction have been developed. Despite having been tested with selected toxicity bioassay panels, some drug candidates that are toxic to a subset of the population are not identified until they are tested or used in humans. In fact, approximately 30% of drug candidates fail at the clinical testing stages due to toxicity issues. Some toxicity-linked drug failures do not manifest until after the drugs are marketed, with catastrophic consequences. Currently, up to US$2 billion are required to develop a single drug, and failures drive up general drug costs (12). Thus, predicting drug toxicity at the earliest stages of development is also critical for the economy of health care (13).

Bioassays for toxicity assessment employ microsomes, cell cultures, or animals (13–15). Numerous assays are typically combined into a panel that can provide a reasonably good prediction of human toxicity (15). Nevertheless, the behavior of a given drug in specific individuals, who may also be taking other drugs, can be nearly impossible to predict via bioassay panels. Although existing toxicity tests are important and useful, their predictive shortcomings are well known. Furthermore, animal and human responses to drugs differ widely and depend on the drug being tested, so animal toxicity studies have variable predictive usefulness.

Approximately a decade ago, our research group identified an unfilled niche for high-throughput, molecularly based screening assays in array formats (16, 17). These assays aimed to predict whether metabolites of drugs and pollutants could react with biomolecules and thus be identified as potentially toxic. We chose damage to DNA as an analytical target because DNA adducts are known toxicity biomarkers (9, 10). Our approach required metabolic enzymes to produce the metabolites in close proximity to DNA. Thus, our methods were developed on the basis of dense DNA-enzyme films on array surfaces or nanoparticles. The latter are biocolloid reactors

that provide samples for LC-MS. Either ECL or LC-MS is used to provide DNA-damage rates that are correlated to the toxicity of compounds and their metabolites (18). In a typical scenario, arrays are used to quickly assess that metabolites react with DNA; then biocolloid reactors generate samples used to elucidate structures and measure the formation rates of individual nucleobase adducts that are responsible for array response. The devices we have developed are inexpensive, are high throughput, and can be employed at early drug-development stages to contribute important toxicity-related reactivity and structure information for test candidates. As far as we know, such specific metabolite reactivity and structural information are not provided by any bioassays. Thus, the approaches described in this review are meant to complement rather than replace existing toxicity bioassays.

The ECL and LC-MS arrays that we developed and discuss below are based on the detection of reactions between DNA and drug or pollutant molecules, or their enzyme-generated metabolites, that produce covalently linked nucleobase adducts (19–21). These adducts are excellent biomarkers for genetic toxicity and cancer risk (22). Reactive metabolites also react with proteins and other biomolecules to yield toxic effects. However, DNA adducts formed by interactions with drug molecules and their metabolites are convenient end points because they are easily measured by ECL and LC-MS.

Bioactivation is a term used to denote reactive metabolite generation by enzymes. When these reactive metabolites cause DNA damage, they are described as genotoxic. Many substrates yield DNA-reactive metabolites, including styrene, polyaromatic hydrocarbons, nitrosamines, aromatic amines, tamoxifen, and other chemotherapeutic agents (23–26). One source of these metabolites comprises the cytochrome (cyt) P450s. The P450s are the major enzymes catalyzing oxidations in the human liver; they account for 75% of all metabolic reactions (**Figure 1**) (27–30). **Figure 2** depicts an accepted catalytic cycle for oxidations by these ferric iron–heme (P-Fe) enzymes that can lead to bioactivation. As discussed below, the toxicity assays that we have developed include these enzymes, so metabolites as well as the parent molecules themselves are featured in the analysis.

Metabolic bioconjugation enzymes have also been included in our toxicity-screening arrays to provide a collection of enzymes that are representative of human or rodent metabolism. Alone or in tandem with cyt P450s, bioconjugation enzymes can deactivate or bioactivate foreign chemicals.

Bioactivation: generation of reactive metabolites by metabolic enzymes

Genotoxicity: refers to toxic effects caused by a reaction between a molecule or its metabolites and DNA

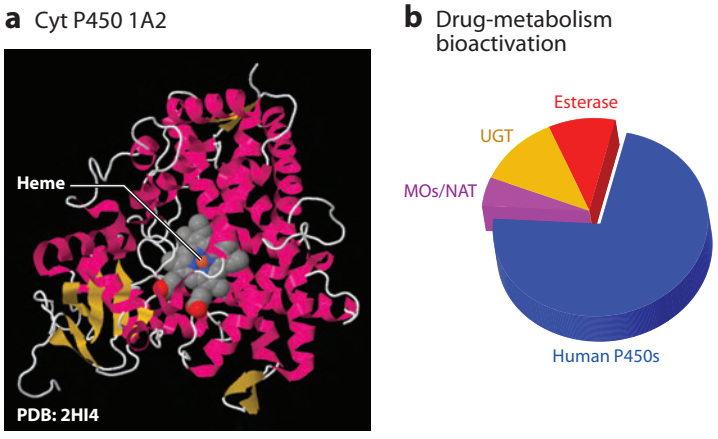

Figure 1

(*a*) Structure of human liver cytochrome (cyt) P450. (*b*) The fraction of existing drugs metabolized by various enzymes. Abbreviations: MO, monooxygenase; NAT, *N*-acetyltransferase; PDB, Protein Data Bank identification; UGT, uridine glutathione transferases.

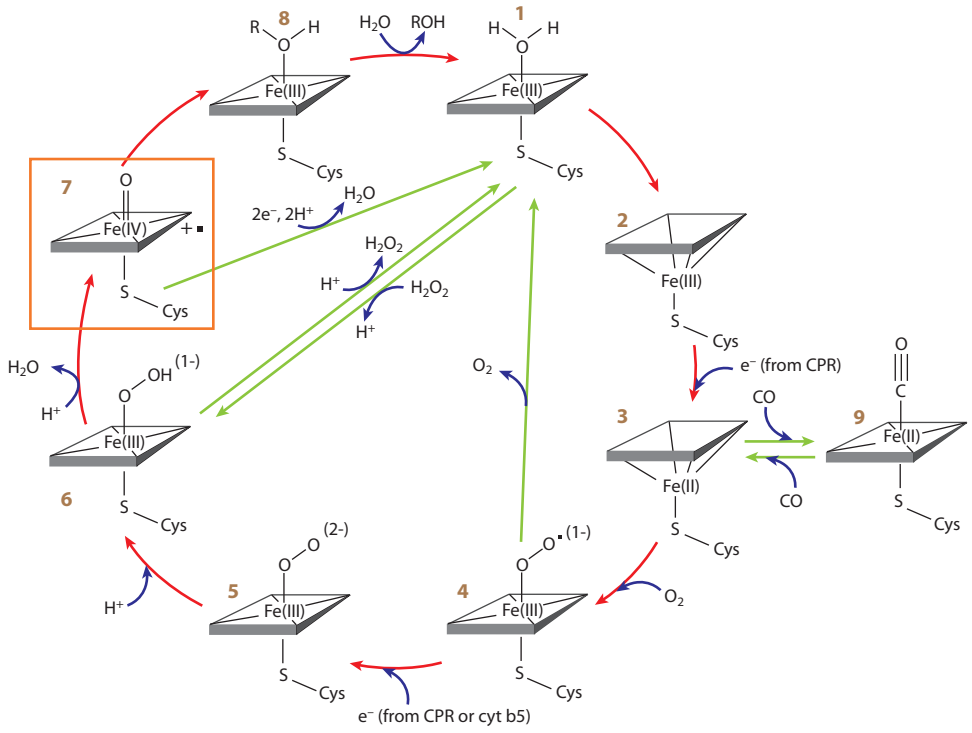

Figure 2

Pathway for cytochrome (cyt) P450–catalyzed metabolic reactions. Initially, the ferric iron–heme (P-Fe) enzyme has water bound to the distal side (***1***) and binds substrate RH to eliminate the water (***2***). Substrate is bound in ***2*** above the iron heme in a hydrophobic pocket. Next, ***2*** is reduced to ***3*** by NADPH-dependent reductase to yield ferrous heme enzyme, which then binds dioxygen to form ferrous dioxygen or ferric superoxy complex (***4***) (31). This complex is reduced to P-Fe(III)-OOH via NADPH reductase to yield ***5*** and is then protonated to ***6***. P-Fe(III)-OOH (***6***) may also be generated by peroxide via the reversible peroxide shunt. Protonation of ***6*** and dioxygen cleavage lead to active heme-iron(IV)-oxo radical cation (**7**), which transfers oxygen to the bound substrate to yield the product ROH. Exposure of ferrous form ***3*** to carbon monoxide (CO) yields P-Fe(II)-CO complex ***9***, which absorbs 450-nm light, hence the name cyt P450 (28). Abbreviation: CPR, cytochrome 450 reductase.

Bioconjugations can follow or precede cyt P450–mediated oxidation to yield reactive metabolites by multienzyme pathways (29, 30). To place our methodologies in context, in the next section we briefly summarize existing and emerging approaches to toxicity screening.

3. ALTERNATIVE TOXICITY-SCREENING ASSAYS AND BIOASSAYS

3.1. Conventional Toxicity Screening

Here, we briefly survey conventional and emerging methods for genotoxicity screening to provide background and comparisons with the approaches that we have developed. Research in this area confirms that DNA damage as a measure of genotoxicity correlates well with overall toxicity and carcinogenicity. Genotoxicity bioassays developed in the 1970s are still in use (14). Assays include the *Salmonella* reverse mutagenicity assay (Ames test) (32), the SOS/*umu* test (29, 33), the micronucleus test (34), the chromosomal aberration test, the mouse lymphoma assay (14), and

the Comet assay (35, 36). Typically, cell growth, protein expression, or electrophoresis tail length (Comet assay) (36) is used to gauge relative genotoxicity. Sensitive derivatization (37); separation (38, 39); and spectral methods, including mass (40, 41), fluorescence (42), IR (43), and Raman (44), have also been developed to detect DNA damage (45).

The widely used Ames assay monitors frameshifts or base-pair substitutions in bacterial DNA that result from exposure to test compounds (32, 46–48). To account for metabolite-mediated toxicity, addition of exogenous liver homogenate (S9 fraction) is often necessary (14, 33), but it can hamper throughput and accuracy (59) and provides limited information about enzyme specificity. Such information can be evaluated by incorporating cyt P450s into supersomes or liver cells and employing colorimetry or chemiluminescence to assay toxicity. Inhibitors are used to identify responsible cyt P450s (49). Idiosyncratic drug reactions (50) and drug-protein interactions have been studied through the use of hepatocytes or microsomal media with radioactive or LC-MS analysis (51). Nucleophilic reactive metabolite trapping, followed by LC-MS, also provides important information (12, 29, 52). Assay throughput and accuracy have been improved through the use of microtiter plates (14, 53–57) in conjunction with green fluorescent protein (GFP)-transformed eukaryotic cells (58–60).

3.2. Emerging Sensor Technologies

Assaying cellular shape as a viability marker is a feature of several emerging toxicity sensors. Exposed cells adopt a less uniform morphology, which affects the transduction surface on which they adhere. Increased light scattering (61) from hepatocytes immobilized on photonic crystals and decreased electron-transfer impedance (62–64) from a cellular-modified microelectrode/microtiter plate apparatus have been monitored following drug exposure. Inhalation toxicants exposed to alveolar cells were studied with fiber evanescent-wave spectroscopy used to monitor mid-IR wavelengths (65). Walt and colleagues (66) developed a genotoxicity assay array using *recA:gfp* or *katG:lux* fusion plasmid–transformed *Escherichia coli* immobilized in fiber-optic microwells. GFP fluorescence or LuxR bioluminescence can be monitored to distinguish genotoxic from oxidative damaging xenobiotics (66–69).

Notingher (70) and Zhang and colleagues (71) used a single-cell gold microarray to monitor apoptosis-related DNA damage with confocal Raman spectroscopy. Miniaturized toxicity assay devices such as the micropatterned Comet array (72) and the Meta-Chip/Data-Chip, which connects cyt P450s with cell lines in a two-dimensional (73) or three-dimensional (74) array apparatus, have the potential to increase toxicity-screening throughput (75–77). The next section includes details of our genotoxicity-screening arrays and assay protocols.

4. IN VITRO DNA-DAMAGE AND TOXICITY SCREENING

4.1. Electrochemical Detection Technologies

Electrochemical methods for DNA-damage and toxicity detection have been developed for more than 50 years (78). In the sections below, we first provide some historical context to show how our toxicity array development has been influenced by this decades-long research effort. We then discuss our approach to measuring the rate of DNA damage by the target compounds and in situ enzyme-generated metabolites.

4.1.1. History and overview Benefits of electrochemical methodologies include speed, low cost, and simplicity of design. Paleček (79) and Fojta (78) pioneered the use of mercury and carbon

electrodes to measure DNA damage. Damaged DNA interacts with mercury electrodes to produce a unique ac voltammetry peak at −1.4 V versus the saturated calomel reference electrode (SCE). Single- and double-strand (ds) breaks, along with enzymatic DNA-repair action, can be detected by monitoring the increase or decrease, respectively, of this voltammetric peak (80–82). Similar electrocatalytic protocols involving OsO_4, 2,2′-bipyridine (bpy) modifications (83), or $Ru(bpy)_3^{2+}$ (84), have also been developed to detect DNA damage.

SCE: saturated calomel reference electrode

Layer-by-layer (LbL) films: ultrathin films constructed one layer at a time

Electrodes modified with short (~20-bp) oligomers have been used to monitor xenobiotic damage at specific DNA sequences (85). Essentially, damage at specific DNA sequences is measured through the use of a hybridization approach in which target DNA is captured by an immobilized probe that exhibits a complementary sequence, followed by exposure to a potential damage-causing xenobiotic molecule. Fluctuations in the redox properties of an electroactive probe bound to DNA before and after exposure to the xenobiotic provide information about DNA damage. Boal & Barton (86) have used this approach to detect oxidative adducts, as have Buzzeo & Barton (87) for abasic sites. Wong & Gooding (88) studied binding of the anticancer drug cisplatin to a specific intrastrand GG sequence. Satterwhite & Hvastkovs (89) used a similar approach to study the binding of benzo[*a*]pyrene (BP) to *p53* gene-sequence oligomers.

4.1.2. Electrochemical sensors for metabolic toxicity In 2001, we began developing sensors for metabolic toxicity by combining metabolic enzymes, DNA, and polyions in thin films on electrodes (90, 91). All of these (and succeeding) approaches produce metabolites in an enzyme reaction step, then monitor DNA damage in an electrochemical detection step. The early sensors and all of our subsequent ECL arrays and LC-MS bioreactors employ a versatile layer-by-layer (LbL) film-fabrication method (92). Films are assembled through electrostatic adsorption of alternately charged layers of DNA and polyelectrolytes, including redox polymers, metabolic enzymes, proteins, and synthetic polyions. These films have excellent stability, and their thickness can be controlled on the nanometer scale.

The typical growth of electrochemical sensor films begins with a negatively charged pyrolytic graphite (PG) disk electrode dipped into an aqueous 1–3 mg liter^{-1} polycation solution. Steady-state adsorption of the polycation is reached within ~20 min (92). After being washed with water, the surface is positively charged because of excess surface polycations (**Figure 3*a***). This electrode is then dipped into a DNA solution, and this newly adsorbed anionic layer reverses the surface charge. Following washing, a positively charged enzyme is then adsorbed. These steps are repeated until the desired number of DNA-enzyme bilayers has been deposited. Adsorption is accomplished by placing single 10–30-μl drops on the sensor electrode, which conserves expensive DNA and enzymes (93). Very stable films are obtained because strong interactions are selected; the strong interactions result from the washing steps' removal of weakly adsorbed molecules.

Quality control of stepwise film assembly can be monitored by quartz crystal microbalance (QCM) weighing, surface plasmon resonance, spectroscopy, voltammetry, and other methods. QCM provides estimates of the amounts of DNA and enzyme in the films. Although the films are fabricated one layer at a time, individual layers are intermixed with their neighbors (92, 93). Layer mixing facilitates toxicity-screening applications by bringing together enzymes and DNA so that the generated reactant molecules are formed in a restricted volume with a very large DNA concentration.

Our toxicity sensors mimic human liver metabolism by combining enzyme bioactivation with resulting DNA damage. All the sensing approaches involve two steps: (*a*) bioactivation of test chemicals by metabolic enzymes in the films and (*b*) measurement of DNA damage from the resulting metabolites (**Figure 3*b***). Our initial electrochemical sensors featured 20–40-nm-thick films containing bacterial cyt $P450_{cam}$. The enzymes were activated by H_2O_2 (**Figure 2**) to produce

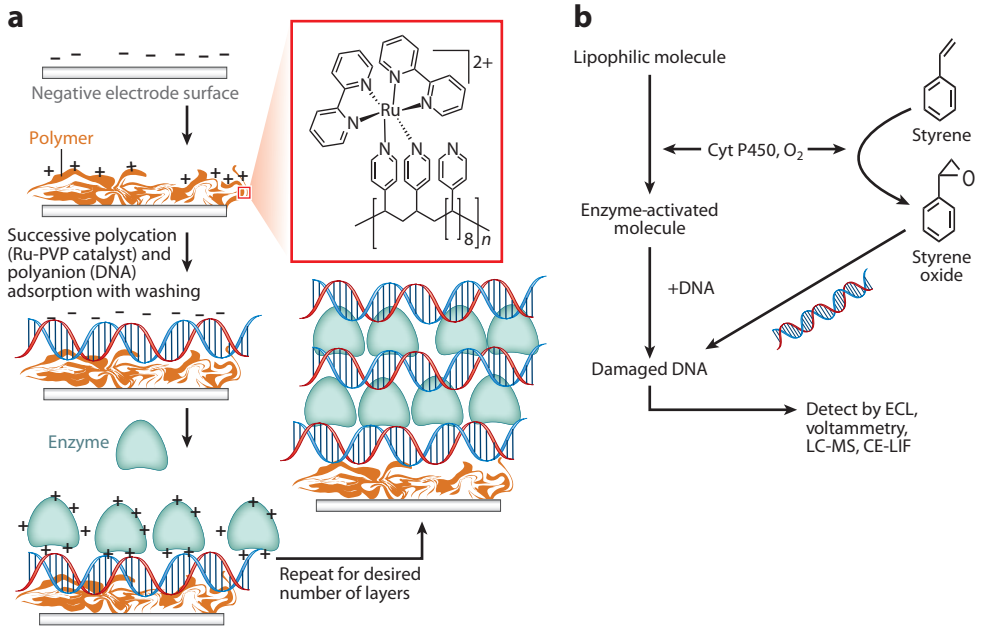

Figure 3

Approaches used to design toxicity sensors and arrays. (*a*) Polyion-DNA-enzyme film formation by the layer-by-layer method. (*b*) Example of a pathway of molecular bioactivation leading to a toxic metabolite that reacts with DNA. Abbreviations: CE-LIF, capillary electrophoresis–laser-induced fluorescence; cyt, cytochrome; ECL, electrochemiluminescence; LC-MS, liquid chromatography–mass spectrometry.

metabolites that react with dsDNA as they diffuse out of the film. Control experiments showed that, under the conditions of these experiments, no DNA damage occurs from H_2O_2 alone; therefore, such damage arises from reactions with metabolites. DNA damage was detected by square-wave voltammetry (SWV) through the use of catalytic oxidation of DNA by dissolved $Ru(bpy)_3^{2+}$ (94). DNA detection is based on the oxidation of guanine, the most easily oxidized DNA nucleobase (78). $Ru(bpy)_3^{2+}$ oxidizes only guanines in DNA by electrochemical catalysis (**Figure 4**) (95).

In our first toxicity-screening sensors, soluble $Ru(bpy)_3^{2+}$ was oxidized by the electrode to yield $Ru(bpy)_3^{3+}$ (**Figure 4*a***), which reacts with DNA to yield guanine radical DNA(G$^{\cdot}$) in a fast proton-coupled chemical step (**Figure 4*b***) (95) that regenerates $Ru(bpy)_3^{2+}$. Peak current increases as the rate of the step in **Figure 4*b*** increases. The chemical damage to the DNA partly unwinds the DNA double helix, making the guanines in the DNA more accessible to $Ru(bpy)_3^{3+}$ and increasing the rate of guanine oxidation, resulting in increases in the SWV peak current. By

a

$$Ru(bpy)_3^{2+} \longrightarrow Ru(bpy)_3^{3+} + e^- \text{ (at electrode)}$$

b

$$Ru(bpy)_3^{3+} + DNA(G) \longrightarrow Ru(bpy)_3^{2+} + DNA(G\bullet) + H^+$$

Figure 4

Pathway for electrocatalytic guanine oxidation by soluble $Ru(bpy)_3^{2+}$.

hydrolyzing the films and measuring the DNA adduct–formation rate using LC-MS (11, 18, 90, 91), we showed that SWV peak current–versus–reaction time plots corresponded to DNA-damage rates. Sensor and LC-MS results also correlated well with animal genotoxicity metrics (9, 96).

TprA: tripropylamine

4.1.3. Single-electrode electrochemiluminescence toxicity sensors. ECL is an electrochemically driven light-emission process that has increased in importance in bioanalysis (4, 5). In many applications, $Ru(bpy)_3^{2+}$ produces visible ECL light through chemical interactions with a sacrificial reductant, such as tripropylamine (TprA), at oxidizing potentials to yield excited-state $[Ru(bpy)_3^{2+}]^*$, which emits light at 610 nm. The mechanism involves reactions of both oxidized and reduced forms of TprA and $Ru(bpy)_3^{2+}$ and depends on concentrations of both. Various ECL-producing mechanisms involving these reactants have been summarized elsewhere (97). $Ru(bpy)_3^{2+}$-labeled DNA using TprA coreactant has been developed into a very sensitive ECL method to detect oligonucleotide hybridization (98–100).

$Ru(bpy)_3^{2+}$ can be incorporated into polymer forms that can be used in LbL films. The Ru-polyvinylpyridine (Ru-PVP) polymer (**Figure 5**) contains $Ru(bpy)_2^{2+}$ sites that catalyze DNA oxidation. Ru-PVP, which features six Ru-N bonds, can be reversibly oxidized on PG electrodes at ~1.2 V versus Ag/AgCl and produces ECL with DNA in thin films (101). A similar polymer known as Ru-Cl-PVP, which features five Ru-N bonds, can be reversibly oxidized at 0.75 V versus SCE and has been used for the electrochemical detection of DNA damage (102), but it does not produce ECL.

In our ECL sensors, TprA is not required because DNA itself acts as the sacrificial reductant. Ru-PVP in DNA films generates ECL when its Ru(II) sites are electrochemically oxidized to Ru(III) sites (101), similar to the ECL reaction involving $Ru(bpy)_3^{2+}$ (see below for discussion of this pathway). We measured ECL by using a sensor coated with a Ru-PVP–enzyme–DNA film positioned directly above an optical fiber that directs light to a photomultiplier (**Figure 6*a***) (101). The sensor measures voltammetry and ECL simultaneously, as has been demonstrated in toxicity-screening applications (103).

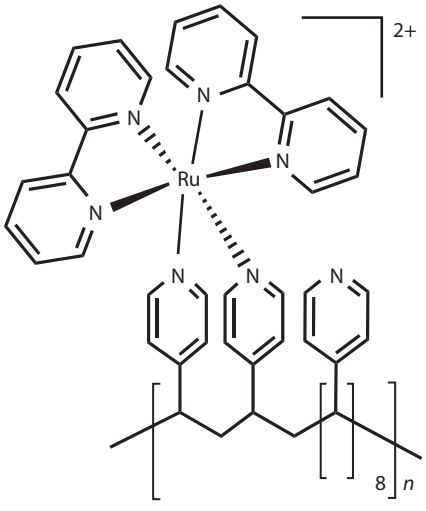

Figure 5

Chemical structure of an electrochemiluminescence-generating Ru(II)-PVP polymer.

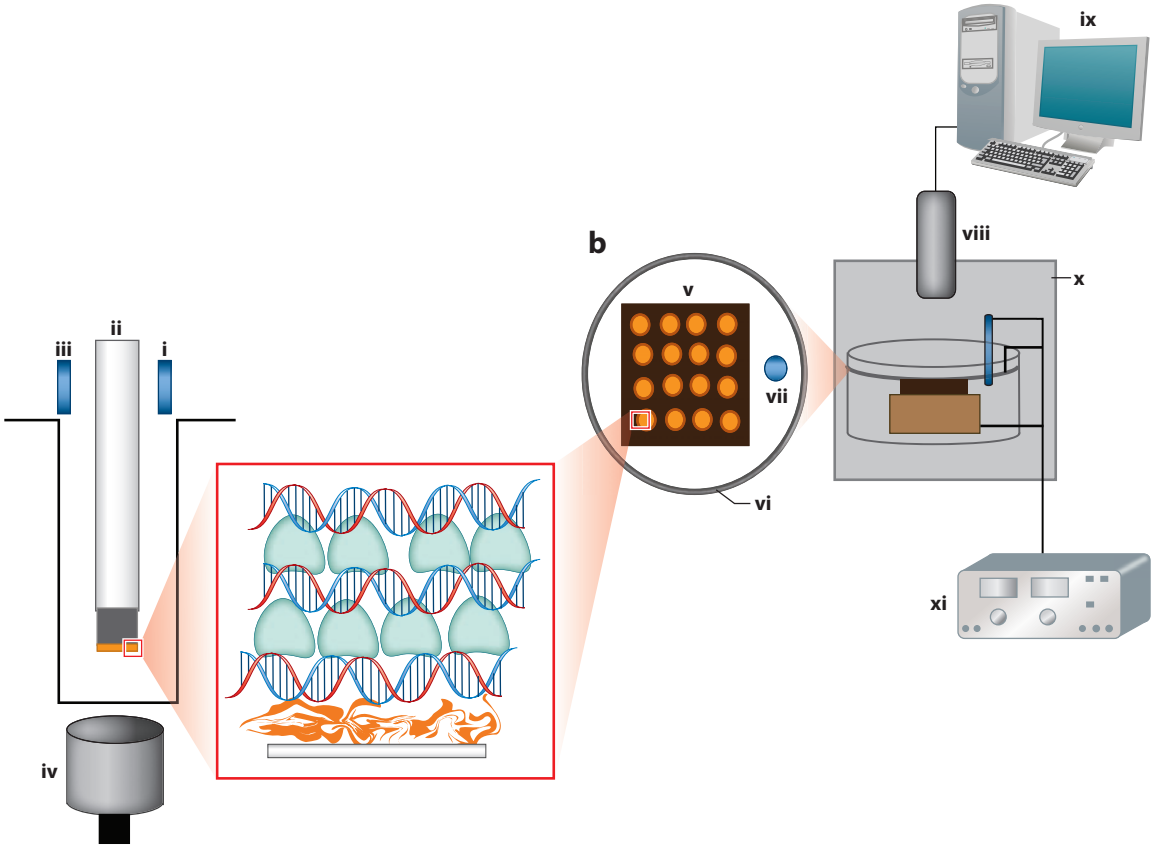

Figure 6

Configurations of electrochemiluminescence (ECL) toxicity sensors. (*a*) A single-electrode sensor coated with DNA–enzyme–Ru-PVP films with (*i*) reference electrodes and (*iii*) counterelectrodes. The sensor is placed above (*iv*) an optical fiber connected to a photomultiplier tube for light detection. (*b*) Array showing (*v*) the pyrolytic graphite chip working electrode; the DNA–enzyme–Ru-PVP spots are shown with Ag/AgCl reference (*vi*) and Pt-wire counterelectrodes (*vii*). For ECL readout, the device is (*x*) placed into a dark box and (*xi*) connected to a potentiostat that applies 1.2 V while (*viii*) a charge-coupled device camera detects the light. (*ix*) A computer is interfaced for data capture and analysis.

All of our ECL-generating sensors feature Ru-PVP–enzyme–DNA films. The ECL coreactants are guanines in the DNA strand (**Figure 7**) (101). Electrochemical oxidation at ~1.2 V versus Ag/AgCl generates Ru(III)-PVP (**Figure 7*a***) that catalytically oxidizes guanines (**Figure 7*b***), thereby producing guanine radicals, $G^{\cdot}$, on the DNA (104). These radicals react with Ru(III)-PVP metallopolymer to produce electronically excited Ru(II)*-PVP (**Figure 7*c***). Alternatively, reaction of Ru(II)-PVP with $G^{\cdot}$ yields Ru(I)-PVP (**Figure 7*d***), which reacts with Ru(III)-PVP to yield Ru(II)*-PVP (**Figure 7*e***). Ru(II)*-PVP, in turn, decays to emit ECL light at 610 nm (**Figure 7*f***). As in the electrocatalytic oxidation of DNA measured by voltammetry, the active Ru(III)-PVP sites gain better access to guanines in partly unfolded, damaged DNA than in intact dsDNA; thus, damaged DNA has an increased formation rate of ECL-emitting Ru(II)*-PVP, and the ECL light output is larger for damaged DNA than for undamaged DNA (see References 94 and 101 for experiments supporting these mechanistic details).

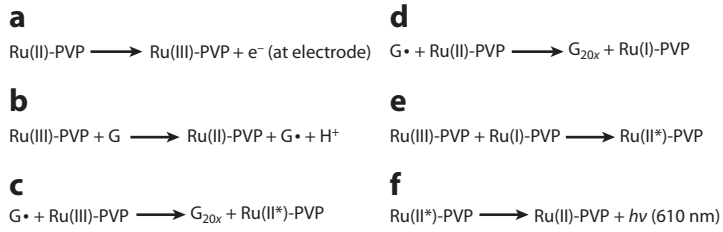

Figure 7

Pathway for electrocatalytic guanine oxidation leading to electrochemiluminescence (ECL) generation from the excited Ru(II)*-PVP polymer.

Individual ECL toxicity sensors that incorporate Ru-PVP provide optical outputs as well as larger voltammetric signals, compared with those provided by sensors that use soluble $Ru(bpy)_3^{2+}$ (103). This finding is consistent with the observation that immobilized Ru-PVP exhibits higher ECL efficiency compared with that of solubilized polymer (105). An individual sensor detected ~3 damaged bases out of 10,000 bases within 1 min of reaction.

5. ELECTROCHEMILUMINESCENCE ARRAYS FOR TOXICITY SCREENING

The single-sensor studies described above eventually led us to pursue the development of a higher-throughput array format for ECL-based toxicity sensors. These arrays were fabricated without multielectrode devices by use of a single conductive chip. Individual DNA–enzyme–Ru-PVP spots are deposited in spatially distinct regions on underlying electrodes that need only be a conducting material. In our ECL arrays (**Figure 6*b***) (106), a 1-inch^2 PG chip is electrically connected to a copper "shoe" via silver epoxy, and the entire underassembly is insulated with acrylic polymer, so only the conductive PG face is exposed. Ru-PVP, DNA, and metabolic enzymes are manually spotted onto demarcated locations on the exposed PG surface. Manual spotting techniques have been used to reproducibly produce 36–50 spot arrays, upon which DNA–Ru-PVP–enzyme spots were clearly visible (106).

When purified enzymes are used, the bioactivation reaction step typically involves deposition of reactants, along with 0.5 mM of H_2O_2, on array spots. Upon completion of the reaction, detection requires submerging the array in pH-5.5 acetate buffer in an open electrochemical cell underneath a charge-coupled device (CCD) camera in a dark box (**Figure 6*b***). A Pt-wire or mesh counterelectrode ring surrounds the outside of the array to achieve a degree of cell symmetry, and the system features an Ag/AgCl reference. ECL is generated by applying 1.25 V versus Ag/AgCl and captured by using the CCD camera during 20-s electrochemical oxidation pulses (107).

5.1. Bioactivation Using Purified Enzymes

ECL arrays with up to 50 spots dramatically increase throughput for toxicity screening. Our initial studies focused on reactive BP metabolites generated from pure cyt P450s; these studies aimed to identify the most effective enzymes in BP metabolism. **Figure 8*a*** shows a single-enzyme analysis using cyt P450 1B1. ECL intensity increased with reaction time. The absence of a change in ECL from controls confirms that the ECL increase is due to reactive BP metabolites. **Figure 8*b*** shows the ECL ratio (ECL at reaction time $t = n$ divided by ECL at $t = 0$) versus time plots. Cyt 1B1 films exposed to BP/H_2O_2 produced ECL increases that were well above background and saturated after ~1 min. Thus, all DNA-damage rate information was obtained within 1 min.

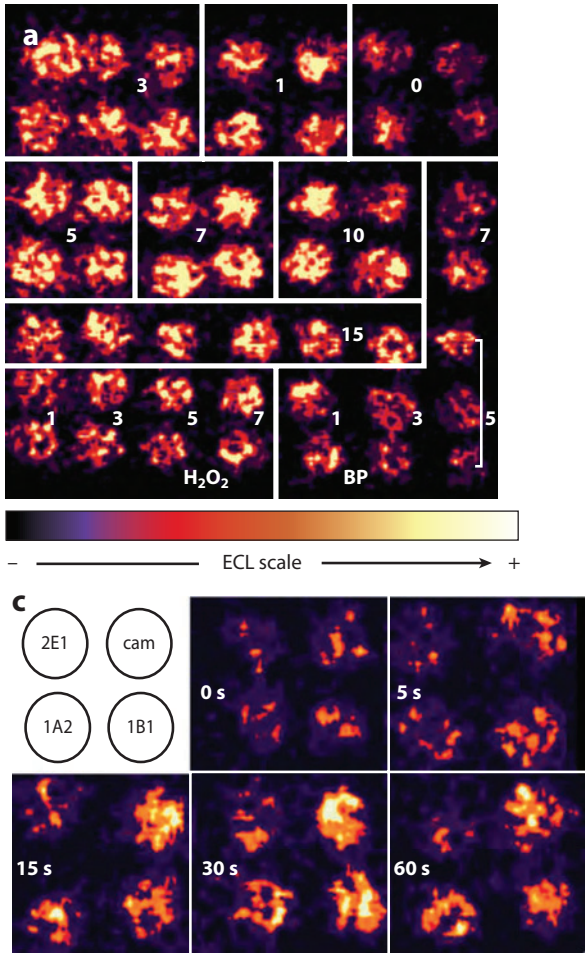

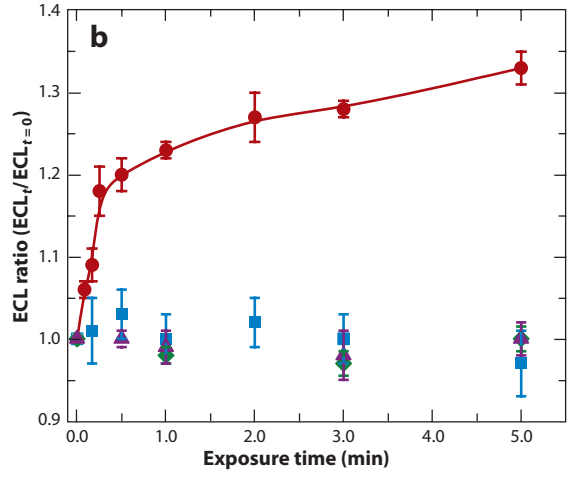

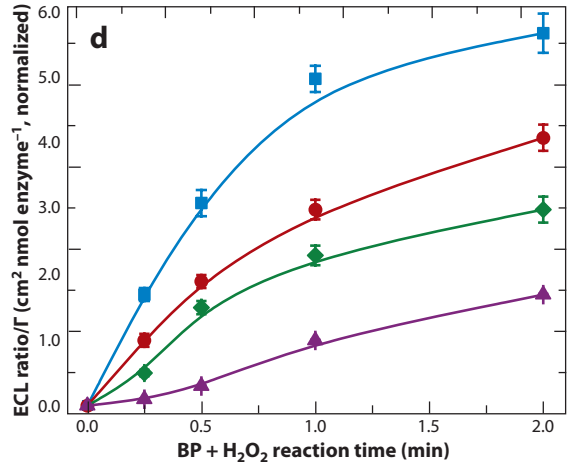

Figure 8

(*a*) Electrochemiluminescence (ECL) array image showing 49 individual Ru-PVP–DNA–cytochrome (cyt) P450 1B1 spots. The boxes show the exposure time (in minutes) to 100 μM of benzo[*a*]pyrene (BP) + 0.5 mM of H_2O_2 or to controls in which the spots were exposed to the individual reagents. (*b*) ECL ratio plot showing the array response for the following reactions: BP + H_2O_2 (*red circles*), BP only (*blue squares*), H_2O_2 only (*green diamonds*), and BP + H_2O_2 + αNF (*purple triangles*). (*c*) Reconstructed simultaneous four-enzyme ECL array. Each spot consisted of Ru-PVP–DNA–denoted enzyme and was exposed to 100 μM of BP + 0.5 mM of H_2O_2 for the denoted time (in seconds). (*d*) Normalized ECL ratio plots demonstrating the signal increase upon 100 μM of BP + 0.5 mM of H_2O_2 exposure for the following: cyt P450 1B1 (*blue squares*), cyt P450 1A2 (*red circles*), cyt P450 cam (*green diamonds*), and cyt P450 2E1 (*purple triangles*). Adapted with permission from Reference 106. Copyright 2007, American Chemical Society.

Figure 8*b* also shows low ECL ratios obtained via αNF, a cyt P450 1B1 inhibitor that prevents BP metabolism (106). This finding demonstrates that an increase in ECL is a consequence of the enzyme reaction.

An array designed to reveal enzymes responsible for the reactive BP metabolites (**Figure 8*c***) included cyt P450s 1B1, 1A2, cam, and 2E1 (106). ECL from cyt P450s 1B1, 1A2, and cam appears to increase more dramatically compared with ECL from cyt P450 2E1. After ECL was normalized for the amounts of enzyme in each film, the order of reactivity was cyt P450 1B1 > 1A2 > cam > 2E1 (**Figure 8*d***), which is consistent with results from previous enzyme kinetic studies.

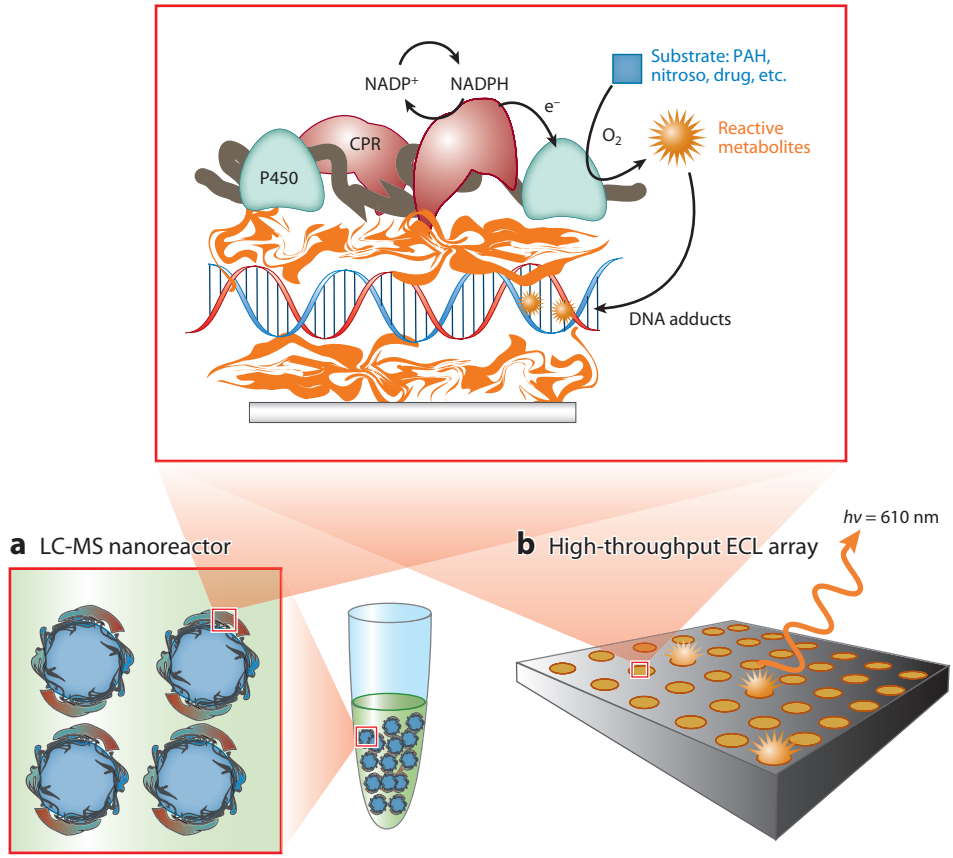

Figure 9

Microsome-DNA films and reactions on (*a*) bioreactors and (*b*) electrochemiluminescence (ECL) array chips. A layer of cationic polymer [e.g., poly(ethyleneimine) or Ru-PVP] is initially deposited (*orange ribbon*), followed by layers of negative DNA, polycation, and microsomes [membrane, brown; cytochrome (cyt) 450 reductase (CPR), red; cytochrome (cyt) P450, green]. NADPH generated by an enzyme reaction in solution reduces CPR, which transfers electrons to cyt P450s. O_2 and cyt P450s can combine to convert the substrate to reactive metabolites that form DNA adducts in the film. ECL is detected with a charge-coupled device camera above the array upon application of +1.25 V versus Ag/AgCl to monitor DNA adduct accumulation. Hydrolysis releases labile DNA adducts from the nanoreactors for capillary liquid chromatography–mass spectrometry (LC-MS) analysis. Abbreviation: PAH, polycyclic aromatic hydrocarbon.

5.2. Bioactivation Using Microsomal Enzymes

The use of isolated enzymes in the arrays can provide specific metabolic information, but these enzymes can be obtained only in limited quantities after lengthy purification processes. Also, activating cyt P450s with peroxide is close to, but not exactly the same as, natural catalytic activation. To eliminate these drawbacks, we began to use rat liver microsomes (RLMs) and single–cyt P450 (bicistronic) membrane fractions as ECL array enzyme sources (108). RLMs are commercially available mixtures of lipids, cyt P450s, and bioconjugation enzymes. Large amounts of cyt P450 bicistronic membrane fractions can be isolated from *E. coli* expression within ~3 days, as opposed to 20–30 days for purified human cyt P450s. RLMs and bicistronic membrane fractions contain cyt

RLM: rat liver microsome

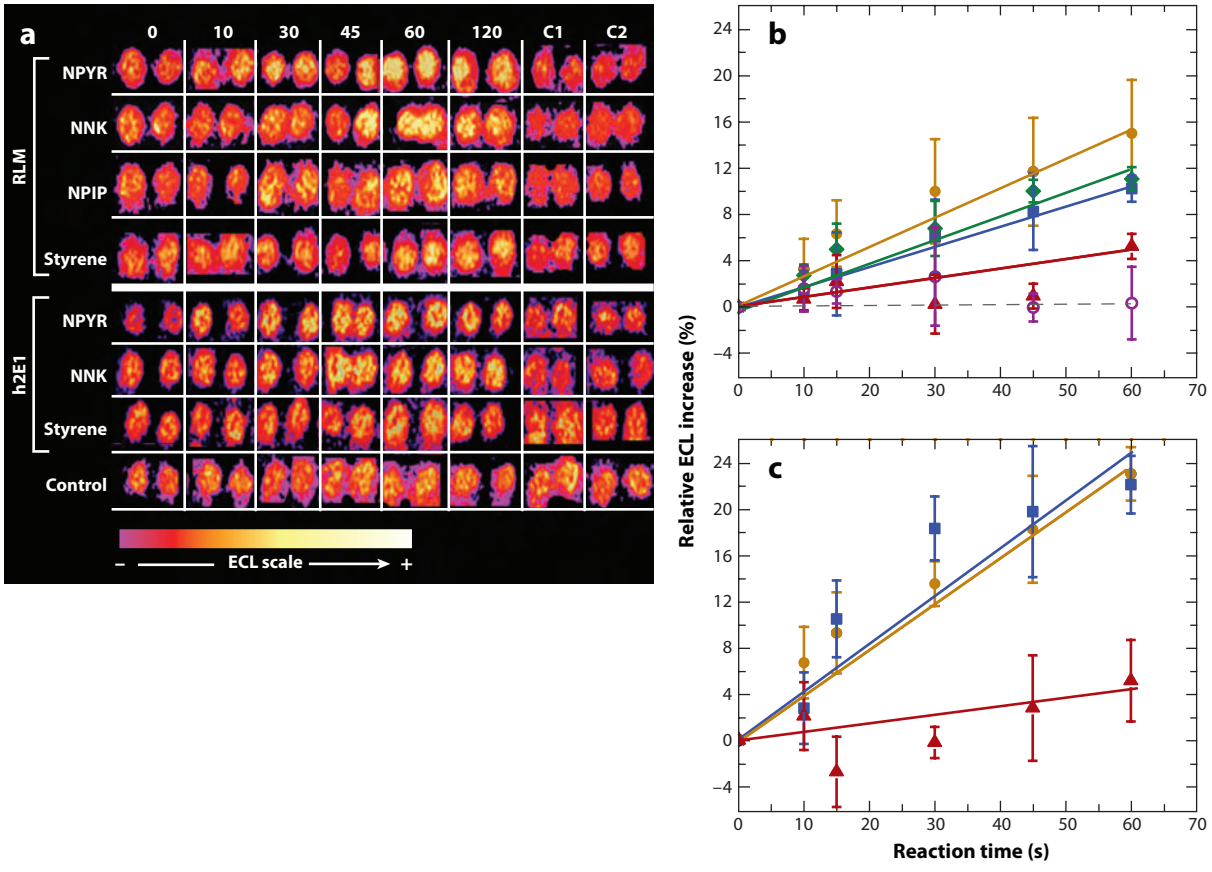

Figure 10

(*a*) Reconstructed electrochemiluminescence (ECL) array demonstrating Ru-PVP–DNA–RLM [or bicistronic cytochrome P450 2E1 (h2E1)] response upon exposure to the denoted substrate (1 mM) in a NADPH generation buffer for the denoted time (in seconds). ECL results for each substrate are from the same array. Control shows an RLM array (the h2E1 array was similar but is not shown) exposed to no reagents. C1, 120-s exposure to NADPH buffer; C2, 120-s exposure to substrate only (no NADPH). Percent ECL increase versus reaction time is shown for (*b*) RLM films and (*c*) h2E1 films exposed to NPYR (*gold circles*), NNK (*blue squares*), NPIP (*green diamonds*), styrene (*red triangles*), and NADPH buffer only (*open purple circles*). Abbreviations: NNK, 4-(methylnitrosoamino)-1-(3-pyridyl)-1-butanone; NPIP, *N*-nitrosopiperidine; NPYR, *N*-nitrosopyrrolidine; RLM, rat liver microsome. Adapted with permission from Reference 108. Copyright 2008, American Chemical Society.

P450 reductase, which allows the activation of enzymes via the natural pathway, using NADPH. **Figure 9** illustrates the use of these enzyme sources for toxicity studies.

Figure 10*a* shows an ECL array in which an RLM or a human cyt P450 2E1 (h2E1) bicistronic fraction was incorporated into Ru-PVP/DNA spots to probe the bioactivation of 4-(methylnitrosoamino)-1-(3-pyridyl)-1-butanone (NNK), *N*-nitrosopyrrolidine (NPYR), and *N*-nitrosopiperidine (109). These spots yielded larger ECL increases than did those treated with styrene, which suggests that *N*-nitroso metabolites have a higher reactivity with DNA. **Figure 10*b–c*** shows ECL ratio increases for RLM and h2E1 arrays.

ECL decreased from RLM and h2E1 arrays exposed to the cyt P450 2E1 inhibitor 4-methyl pyrazole and NPYR, which demonstrates that the inhibitor blocks the formation of reactive metabolites (108). Because cyt P450 2E1 is the only isoform present in h2E1 films, this result

demonstrates that the cyt P450 2E1 enzyme is the predominant cause of the formation of reactive NPYR metabolites.

5.3. Correlations with Animal Toxicity

Slopes of the initial ECL increase versus reaction time (**Figure 10*b–c***) are related to substrate-specific enzymatic bioactivation turnover rates. This finding was confirmed with LC-UV-MS in a study of individual nucleobase adduct–formation rates (108). These data gave good correlations with the rodent median toxic dose (TD_{50}), which monitors the propensity for chemically induced liver tumor formation. The three *N*-nitroso compounds exhibit similar TD_{50} values (~1.6 mg per kilogram of body weight per day), whereas styrene has a larger TD_{50} value (23 mg per kilogram of body weight per day). All three *N*-nitroso compounds yielded similar ECL and LC-UV-MS turnover rates, but styrene was less active and showed a lower DNA-damage rate. This inverse correlation to rat TD_{50} demonstrated the consistency of our results (108) with in vivo genotoxicity. Overall, microsomes and bicistronic membrane fractions provide convenient and versatile enzyme sources for ECL and LC-MS arrays to create accurate, high-throughput tools to predict genotoxicity. These arrays measure relative DNA adduct–formation rates under assay conditions. More reliable human toxicity prediction should be achieved when these methods are combined with complementary bioassays for DNA damage and cytotoxicity.

6. BIOCOLLOID REACTORS AND LIQUID CHROMATOGRAPHY–MASS SPECTROMETRY DETECTION

The ECL arrays described above may indicate that a metabolite reacts with DNA at a rate suggesting toxicity, but they provide no information about the structures of the reaction products. Metabolites may be alkylating agents that form DNA adducts (110) by attack at nucleobase nitrogen and oxygen sites (**Figure 11**). We therefore developed LC-MS approaches as sensitive

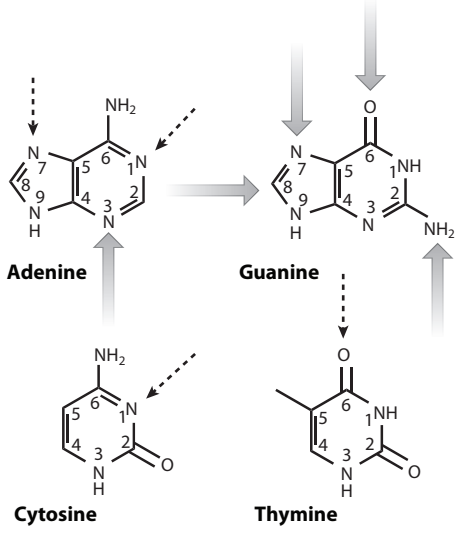

Figure 11

DNA bases showing possible alkylation sites. Larger arrows denote more biologically relevant damage sites; smaller arrows denote less relevant sites.

methods to detect DNA adducts, and these approaches provide information about chemical structures and rates of formation (9, 10, 111). We combined electrospray ionization MS and capillary LC with online preconcentration for ultrasensitive detection of nucleobase adducts in small hydrolyzed DNA samples (11, 18). This approach can be used to further examine ECL array hits to provide metabolite-nucleobase adduct structures and rates of formation.

Guanine is the most reactive DNA base, and nucleophiles often form adducts at N7-guanine. Neutral thermal hydrolysis can be used to selectively eject mainly N7-guanine and N3-adenines (112) by heating the DNA. When separated from intact DNA, a sample enriched in these adducts is produced and is accompanied by far fewer native nucleobases than from acid or enzymatic hydrolysis (11, 113). Any of these hydrolysis methods can be used to obtain nucleobase adducts for LC-MS analysis. Thermal hydrolysis is the simplest and fastest method, but it does not allow for the enrichment of all adducts.

LC-MS studies confirmed that our electrochemical sensors (described above) actually measure DNA damage (11, 113, 114). Initially, DNA films on carbon cloth were reacted with damage agents, the DNA was hydrolyzed, and individual DNA adduct–formation rates were measured. N7-guanine adduct–formation rates measured by LC-MS correlated well with the slopes of electrochemical SWV sensor response versus reaction time for selected carcinogens. These studies clearly established that the sensor-response slopes measure relative DNA-damage rates.

We improved reaction efficiency over that in solution by using DNA-enzyme LbL films on 500-nm-diameter silica biocolloids (107). The reactions catalyzed by these coated particles were monitored by LC-MS on the same timescale on which the ECL arrays operate. ECL arrays and biocolloid LC-MS analyses provide complementary tools for toxicity studies. ECL arrays provide rapid, inexpensive, high-throughput screening. The biocolloid LC-MS approach is somewhat more time consuming and costly compared with ECL arrays but it provides information about structures and metabolite- and nucleobase adduct–formation rates (18). These biocolloid reactors combine large active surface areas with tiny solution volumes to conserve biomolecules and obtain large product concentrations per unit time (115).

We created enzyme-DNA biocolloid reactors for the oxidation of NNK (see the previous section) by using the human cytochrome P450 h2E1 preparation. NNK was oxidized with h2E1 biocolloids activated by 1 mM of H_2O_2. NNK metabolites underwent hydrolysis to 4-hydroxy-1-(3-pyridyl)-butanone, which reacted primarily at N7-guanine (**Figure 12**). **Figure 13*a*** shows an LC-MS/MS (tandem mass spectrometry) chromatogram, and **Figure 13*b*** depicts a single-reaction monitoring (SRM) mass spectrum showing product mass-to-charge (*m/z*) peaks after reaction and neutral thermal hydrolysis to release N7-guanine adducts (107). The *m/z* 299 → 152 peak is consistent with the formation of N7-pyridyloxobutylated guanine (**Figure 12**), which produces *m/z* 152 upon fragmentation. The multiple peaks in **Figure 13*a*** arise from positional isomers.

Figure 13*c* shows that the integrated peak area increases with reaction time. Thus, the specific metabolite-formation rate correlates well with the rate of ECL increase when arrays consisting of similar components are used (116). In general, DNA-enzyme biocolloids efficiently produce products to elucidate metabolite and/or DNA adduct–formation rates and structures via LC-MS. In addition, biocolloids provide a platform that can also be used to study enzyme inhibition (117).

As we did in ECL arrays, we used microsomes and bicistronic membrane fractions as enzyme sources on biocolloid reactors. Initial studies compared the performance of RLMs with that of singly expressed h2E1 preparations. Cyt P450s in the microsomes were activated via the natural NADPH reductase cycle (108). LbL biocolloids were formed with architecture poly(ethyleneimine)-DNA-RLM (or h2E1). These particles were reacted with *N*-nitroso substrates (see above). Individual nucleobase adducts were formed on the biocolloids, then released following neutral thermal hydrolysis of the DNA.

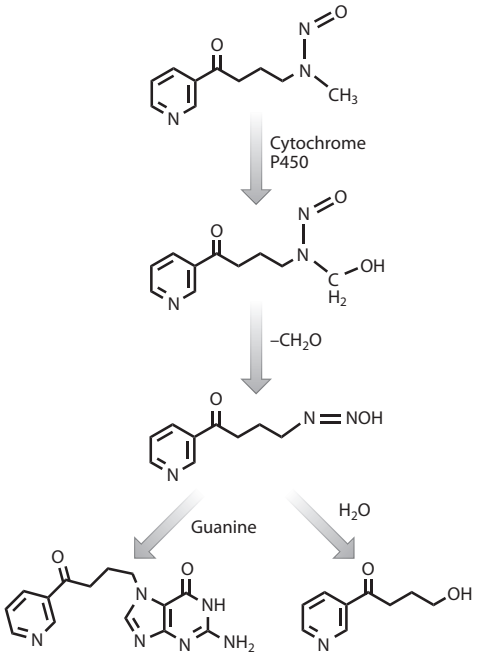

Figure 12

NNK [4-(methylnitrosoamino)-1-(3-pyridyl)-1-butanone] bioactivation pathway by cytochrome P450 enzymes leading to N7-guanine adductor and 4-hydroxy-1-(3-pyridyl)-butanone.

Figure 14 shows SRM MS chromatograms of major guanine adducts on microsome-DNA nanoreactors. The amounts of guanine adducts increased linearly with reaction time over several minutes (**Figure 14*d***) for h2E1 and RLM biocolloids. This finding suggests that reactive metabolites accumulated within the microsome films and produced DNA adducts, consistent with ECL array results. These experiments also confirm that cyt P450 2E1 is an important enzyme in

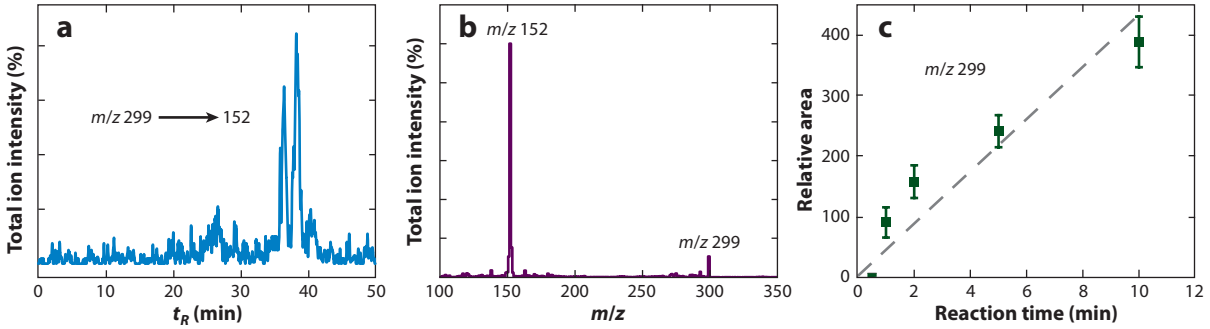

Figure 13

Capillary liquid chromatography–tandem mass spectrometry results for NNK [4-(methylnitrosoamino)-1-(3-pyridyl)-1-butanone] reaction medium catalyzed by DNA–cytochrome P450 2E1 microbeads in pH-5.5 buffer. (*a*) Chromatogram after a 15-min reaction. (*b*) Mass spectrum analyzed by single-reaction monitoring (*m/z* 299 → 152) of the same sample as in panel *a*. (*c*) Influence of reaction time on total integrated area of the peaks in panel *a* at $t_R = 37$. Error bars represent standard deviations. Adapted with permission from Reference 107. Copyright 2008, American Chemical Society.

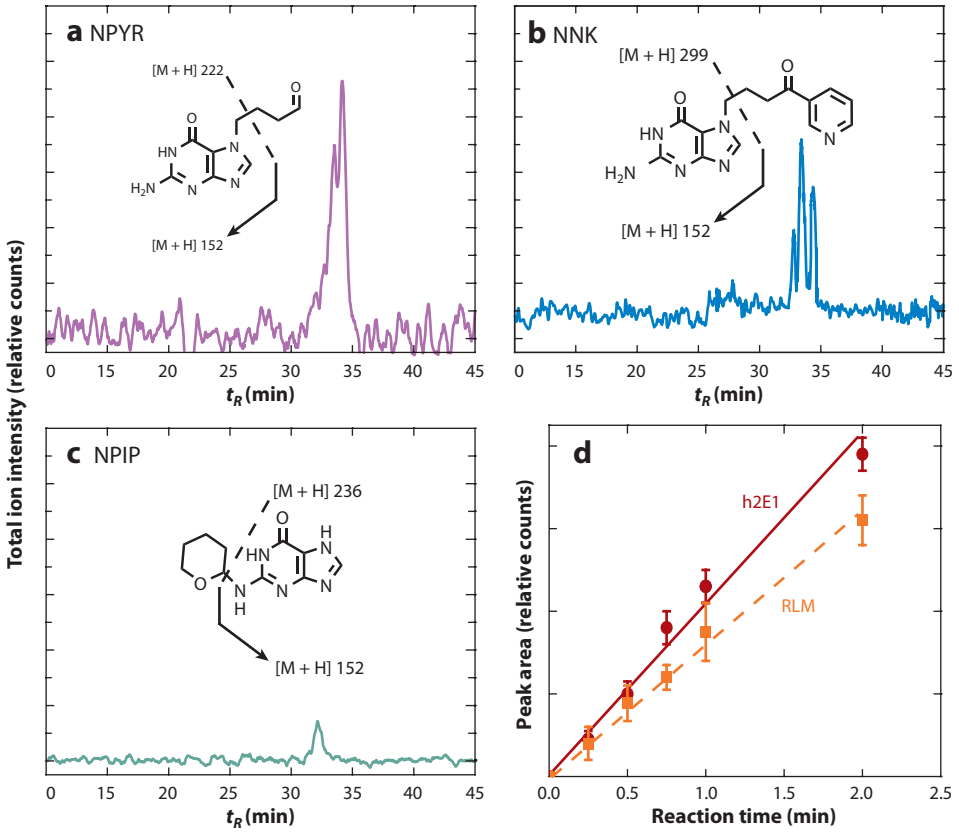

Figure 14

Single-reaction monitoring mass spectrometry chromatograms measuring total ion current for the predominant guanine adduct produced via exposure of (*a*) *N*-nitrosopyrrolidine (NPYR), (*b*) 4-(methylnitrosoamino)-1-(3-pyridyl)-1-butanone (NNK), and (*c*) *N*-nitrosopiperidine (NPIP) to rat liver microsome (RLM)-DNA films on silica nanospheres, followed by DNA hydrolysis. (*Insets*) Examples of relevant guanine adducts and fragmentation patterns consistent with each chromatogram. (*d*) Integrated UV diode array measured peak area increase for NPYR-guanine adducts with reaction time from both RLM and cytochrome P450 h2E1 films. Adapted with permission from Reference 108. Copyright 2008, American Chemical Society.

N-nitroso metabolism because the rates of formation are similar for h2E1 and multiple-enzyme RLMs (108). As discussed above, the slopes of identified adducts versus reaction time correlate well with relative ECL array turnovers and TD_{50}.

We also designed a high-throughput 96-well-plate format for biocolloid reactors coupled with LC-MS. The first example was designed for drug-metabolism profiling (118). Human liver microsomes (HLMs), RLMs, and h3A4 bicistronic microsomes were used to provide a broad range of enzyme biocolloids placed in different wells to simultaneously run many reactions (**Figure 15**). Filters in the bottom of each reaction well allowed for the collection of samples for LC-MS upon completion of the enzyme reaction.

This high-throughput system was used to study diclofenac, troglitazone, and raloxifene metabolism through the observation of known oxidation and bioconjugation pathways as well as turnover rates (118). Enzyme turnover rates obtained via microsomal biocolloids in 96-well

HLM: human liver microsome

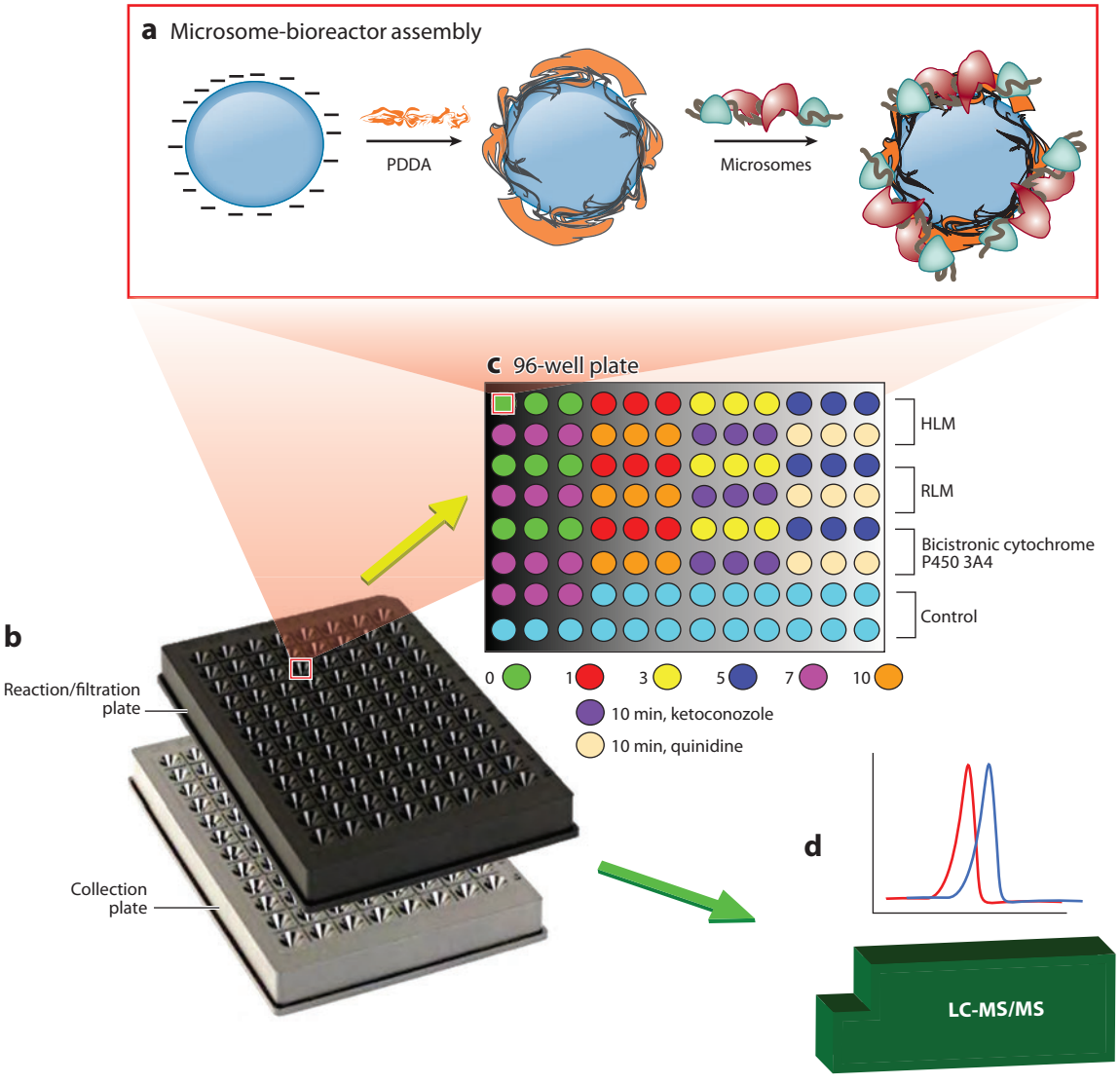

Figure 15

Features of the bioanalytical system for in vitro metabolic profiling. (*a*) Bioreactor assembly. A layer of the cationic polymer polydiallyldimethylammonium chloride (PDDA) was initially deposited on silica nanoparticles, followed by a layer of oppositely charged microsomes. (*b*) A reaction/filtration 96-well plate equipped with 10,000 Da–cutoff mass filters showing the liquid chromatography–mass spectrometry (LC-MS)-ready sample-collection plate underneath. (*c*) Schematic illustration of simultaneous enzyme reaction design featuring a 96-well plate. (*d*) LC-MS/MS (LC–tandem mass spectrometry) analysis with an autosampler. Abbreviations: HLM, human liver microsome; RLM, rat liver microsome.

plates were two- to threefold larger compared with those obtained via conventional microsomal dispersions, probably because of better accessibility of the enzymes to reactants. We found a similar enhancement by using bioreactor particles in manual experiments (117). This system was also used to investigate cyt P450 3A inhibition with ketoconazole and enzyme acceleration with quinidine (118).

The 96-well-plate system was extended to produce DNA adducts for LC-MS (119). Magnetic particles coated with cytosol-microsome-DNA films provided representative cyt P450s and bioconjugation enzyme complements (120). This approach facilitated simple, rapid product generation and hydrolysis through the use of magnetic particle manipulation for solution exchange and filtration. In proof-of-concept studies, we identified the major DNA adducts from ethylene dibromide, *N*-acetyl-2-aminofluorene, and styrene. The metabolism of *N*-acetyl-2-aminofluorene features tandem reactions of *N*-acetyltransferase and cyt P450. Relative DNA adduct–formation rates correlated well with rat TD_{50} for these three compounds (119).

7. TAMOXIFEN CASE STUDY

Through the use of enzyme sources from humans and animals, the technologies described above can be employed to assess species differences in metabolism that may influence toxicity. To demonstrate this concept, we used ECL arrays and biocolloid LC-MS methods to identify rodent toxicity– and human toxicity–related metabolism differences for the breast cancer drug tamoxifen. Tamoxifen causes liver tumors in rats (121), but there is only a small risk of such an outcome in humans (122). We compared the differences in rodents versus humans by using ECL arrays and biocolloid reactors featuring RLMs and HLMs (123).

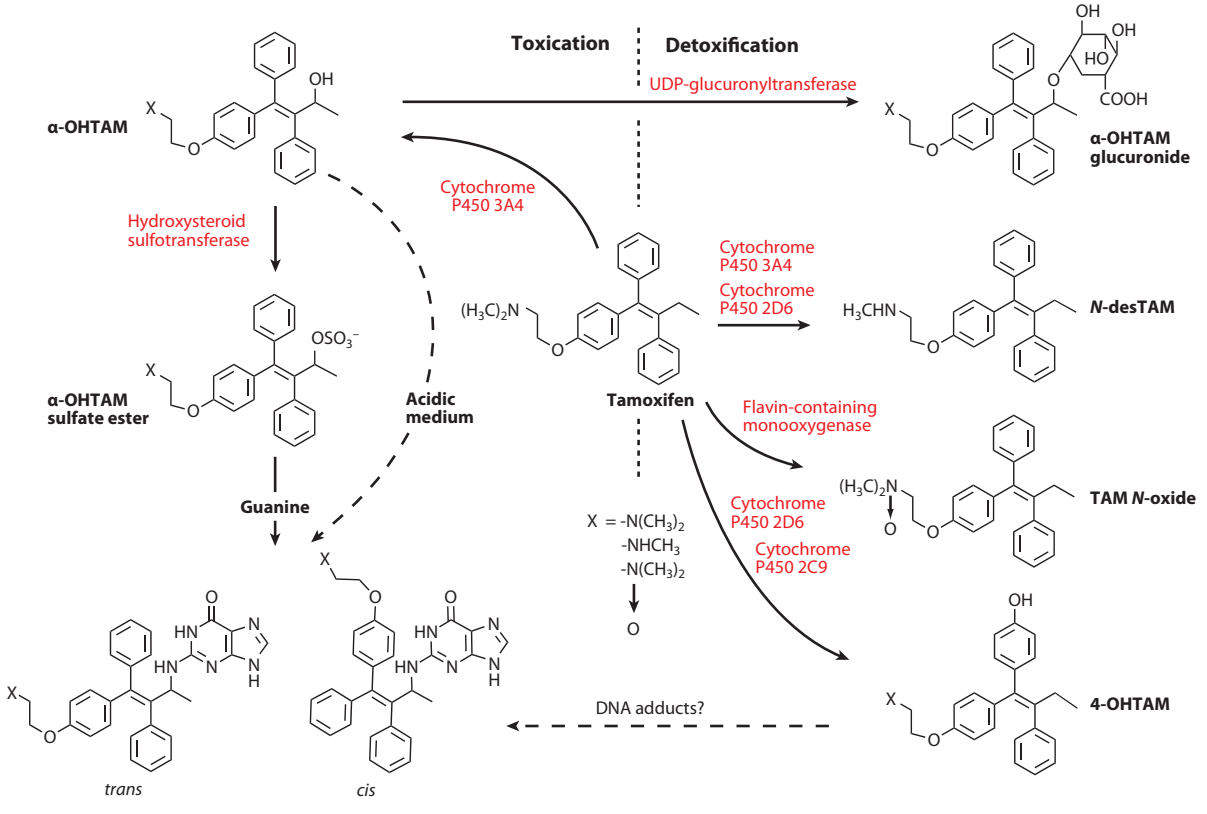

Figure 16

Possible pathways for tamoxifen (TAM) metabolism. Abbreviation: α-OHTAM, 4-hydroxytamoxifen.

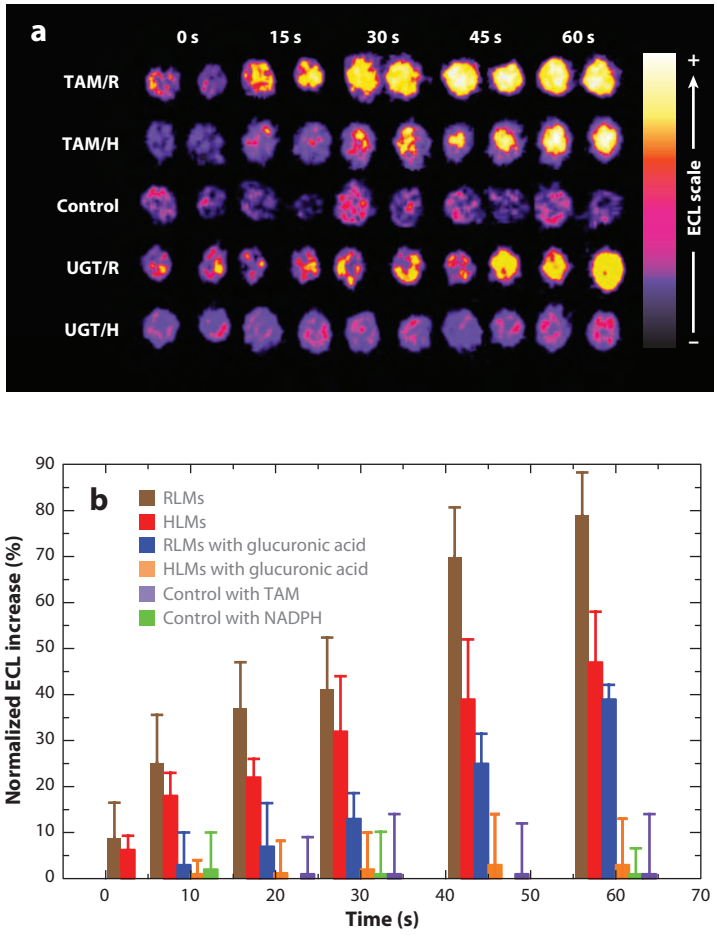

Figure 17

Electrochemiluminescence (ECL) array data for tamoxifen (TAM). (*a*) ECL from spots of Ru-PVP–DNA–rat liver microsomes (RLMs; labeled TAM/R) or Ru-PVP–DNA–human liver microsomes (HLMs; labeled TAM/H) exposed to 25 μM of TAM through enzymatic NADPH regeneration for the denoted time (in seconds). The control was an identical array exposed to 25 μM of TAM, but not NADPH. The detoxication pathway was examined in the presence of 3 mM of UDP-glucuronyltransferase (UGT) in a UGT-catalyzed reaction. Spots with RLM and HLM films were labeled UGT/R and UGT/H, respectively. (*b*) Normalized ECL increase (in minutes per milligram per microsome) for RLMs (*brown*), HLMs (*red*), RLMs with 3 mM of glucuronic acid (*blue*), HLMs with 3 mM of glucuronic acid (*orange*), control incubations with 25 μM of TAM only (*purple*), and control with the NADPH-regenerating system only (*green*). Adapted with permission from Reference 121. Copyright 2009, American Chemical Society.

The metabolic chemistry of tamoxifen involves cyt P450s and bioconjugation enzymes (**Figure 17**). The ECL array image in **Figure 17*a*** is characteristic of in vitro bioactivation when array spots are exposed to tamoxifen and NADPH (**Figure 17*a***) (123). A 1.7-fold-larger ECL turnover rate for RLMs compared with that of HLMs reflects a faster DNA adduct formation for the RLM.

UGT: uridine glutathione transferase

Detoxification mediated by UDP-glucuronyltransferase (UGT) is a major tamoxifen-elimination route that involves glucuronic acid bioconjugation or *O*-glucuronidation to 4-hydroxytamoxifen (α-OHTAM or 4-OHTAM), which reduces the subsequent DNA-damaging

availability (**Figure 16**). HLMs exhibit elevated glucuronidation activity toward α-OHTAM (124). Cofactor UDPGA inclusion in the enzyme reaction produced a much larger ECL decrease when using HLMs versus RLMs (**Figure 17*a***). Results suggest that the rates of DNA adduct formation are slower when UGT-catalyzed bioconjugation is active. These results reflect a better relative UGT bioconjugation efficiency in competition with DNA damage for HLMs than for RLMs (123).

Toxicity hits identified using ECL arrays were followed up by LC-MS/MS of the reaction-product mixture by use of biocolloid reactors. We obtained relative α-(N2-deoxyguanosinyl)tamoxifen–formation rates (120) and found twofold- to fivefold-faster formation of α-OHTAM, 4-OHTAM, and tamoxifen *N*-oxide for RLMs compared with HLMs. The higher formation rate of reactive metabolites may be responsible for the larger ECL turnover rate for RLMs compared with HLMs when bioconjugation is inactive. A better HLM-detoxifying ability was confirmed through the use of glucuronyltransferase and UDP–glucuronic acid. Higher HLM-detoxication rates correlate with a lower risk of tamoxifen-induced human liver carcinoma.

8. SUMMARY AND PROSPECTIVE

This review describes new array methods utilizing enzyme-DNA films to screen chemicals and drug candidates for reactive metabolites on the basis of DNA-damage end points measured by ECL and LC-MS. ECL arrays provide rapid screening, and the biocolloid reactor LC-MS approach provides valuable follow-up information about chemical structures and formation rates for ECL hits. These technologies are currently being developed into higher-throughput versions that take advantage of modern robotics, microfluidics, and materials-printing devices. The future appears bright for incorporation of these technologies into high-throughput chemical and drug toxicity screening. Chemical information obtained through these techniques and integrated with bioassays should enable more informed decision making with regard to chemical and drug candidates. Furthermore, elucidation of toxic-reaction chemistry may facilitate synthetic efforts to design toxicity out of drugs while retaining the desired pharmacological effects.

SUMMARY POINTS

1. The need for new toxicity-screening tools that complement existing bioassays is highlighted by the facts that ~30% of drug candidates fail at clinical testing stages due to toxicity and that some toxicity issues do not manifest until after the drugs are marketed.
2. The new two-tier methodology for screening is based on electrochemiluminescence (ECL) arrays to find toxicity hits, followed with biocolloid reactors and LC-MS/MS for structure and relative DNA-damage rate determinations.
3. DNA-damage rates correlate with rodent genotoxicity metrics.
4. In addition to predicting possible toxic species in vivo, ECL array and biocolloid reactor screening can establish which enzymes are the most important in forming toxic metabolites and can elucidate different genotoxicity pathways between species.

DISCLOSURE STATEMENT

The authors are not aware of any affiliations, memberships, funding, or financial holdings that might be perceived as affecting the objectivity of this review.

ACKNOWLEDGMENTS

The authors' research on toxicity screening was financially supported by U.S. Public Health Service grant ES03154 from the National Institute of Environmental Health Sciences, National Institutes of Health. The authors thank their coauthors of joint publications, without whose excellent contributions this research would not have been possible.

LITERATURE CITED

1. Ramsay G, ed. 1998. *Commercial Biosensors*. New York: Wiley
2. Palaček E, Scheller F, Wang J, eds. 2005. *Electrochemistry of Nucleic Acids and Proteins—Towards Electrochemical Sensors for Genomics and Proteomics*. Amsterdam: Elsevier
3. Davis J, ed. 2009. *Engineering the Bioelectronic Interface*. Cambridge, UK: R. Soc. Chem.
4. Debad JB, Glezer EN, Leland JK, Sigal GB, Wholstadter J, Leland JK. 2004. Clinical and biological application of ECL. In *Electrogenerated Chemiluminescence*, ed. AJ Bard, pp. 359–96. New York: Marcel Dekker
5. Forster RJ, Bertoncello P, Keyes TA. 2009. Electrogenerated chemiluminescence. *Annu. Rev. Anal. Chem.* 2:359–85
6. Ackermann BL, Berna MJ, Eckstein JA, Ott LW, Chaudhary AK. 2008. Current applications of liquid chromatography/mass spectrometry in pharmaceutical discovery after a decade of innovation. *Annu. Rev. Anal. Chem.* 1:357–96
7. Hanash SM, Pitteri SJ, Faca VM. 2008. Mining the plasma proteome for cancer biomarkers. *Nature* 452:571–79
8. Hawkridge AM, Muddiman DC. 2009. Mass spectrometry–based biomarker discovery: toward a global proteome index of individuality. *Annu. Rev. Anal. Chem.* 2:265–77
9. Appruzzese WA, Vouros P. 1999. Analysis of DNA adducts by capillary methods coupled to mass spectrometry: a perspective. *J. Chromatogr. B* 794:97–108
10. Farmer PB, Brown K, Tompkins E, Emms VL, Jones DJL, et al. 2005. DNA adducts: mass spectrometry methods and future prospects. *Toxicol. Appl. Pharmacol.* 207:S293–301
11. Tarun M, Rusling JF. 2005. Measuring DNA nucleobase adducts using neutral hydrolysis and liquid chromatography–mass spectrometry. *Crit. Rev. Eukaryotic Gene Expr.* 15:295–315
12. Caldwell GW, Yan L. 2006. Screening for reactive intermediates and toxicity assessment in drug discovery. *Curr. Opin. Drug Discov. Dev.* 9:47–50
13. Nasser AEF, Kamel AM, Clarimont C. 2004. Improving the decision making process in structural modification of drug candidates: reducing toxicity. *Drug. Dev. Today* 9:1055–64
14. Kramer JA, Sagartz JE, Morris DL. 2007. The application of discovery toxicology and pathology towards the design of safer pharmaceutical lead candidates. *Nat. Rev. Drug Discov.* 6:636–49
15. Mayne JT, Ku WW, Kennedy SP. 2006. Informed toxicity assessment in drug discovery: systems-based toxicology. *Curr. Opin. Drug Discov. Dev.* 9:75–83
16. Stoll D, Bachmann J, Templin MF, Joos TO. 2004. Microarray technology: an increasing variety of screening tools for proteomic research. *Drug Discov. Today Targets* 3:24–31
17. Rusling JF, Hvastkovs EG, Schenkman JB. 2007. Toxicity screening using biosensors that measure DNA damage. *Curr. Opin. Drug Discov. Dev.* 10:67–73
18. Rusling JF, Hvastkovs EG, Schenkman JB. 2009. Screening for reactive metabolites using genotoxicity arrays and enzyme/DNA biocolloids. In *Drug Metabolism Handbook*, ed. A Nassar, PF Hollenburg, JJ Scatina, pp. 307–40. Trenton, NJ: Wiley
19. Jacoby WB, ed. 1980. *Enzymatic Basis of Detoxification*, Vol. I/II. New York: Academic
20. Friedberg EC. 2003. DNA damage and repair. *Nature* 421:436–40
21. Schärer OD. 2003. Chemistry and biology of mammalian DNA repair. *Angew. Chem. Int. Ed.* 42:2946–74
22. DH Phillips, Farmer PB, Beland FA, Nath RG, Poirier MC, et al. 2000. Methods of DNA adduct determination and their application to testing compounds for genotoxicity. *Environ. Mol. Mutagen.* 35:222–33

23. Bond JA. 1989. Review of the toxicology of styrene. *Crit. Rev. Toxicol.* 19:227–49
24. Umemoto A, Komaki K, Monden Y, Suwa M, Kanno Y, et al. 2001. Identification and quantification of tamoxifen-DNA adducts in the liver of rats and mice. *Chem. Res. Toxicol.* 14:1006–13
25. Pfeifer GP, Denissenko MF, Olivier M, Tretyakova N, Hecht SS, et al. 2002. Tobacco smoke carcinogens, DNA damage and p53 mutations in smoking-associated cancers. *Oncogene* 21:7435–51
26. Cavalieri EL, Rogan EG, Devaneshan PD, Cremonesi P, Cerny RL, et al. 1990. Binding of benzo[*a*]pyrene to DNA by cytochrome P450 catalyzed one-electron oxidation in rat liver microsomes and nuclei. *Biochemistry* 29:4820–27
27. Schenkman JB, Greim H, eds. 1993. *Cytochrome P450.* Berlin: Springer. 1st ed.
28. Ortiz de Montellano PR, ed. 2005. *Cytochrome P450.* New York: Kluwer/Plenum. 3rd ed.
29. Liebler DC, Guengerich FP. 2005. Elucidating the mechanisms of drug-induced toxicity. *Nat. Rev. Drug Discov.* 4:410–20
30. Ioannides C, Lewis DFV. 2004. Cytochrome P450 in the bioactivation of chemicals. *Curr. Top. Med. Chem.* 4:1767–88
31. Guengerich FP. 2008. Cytochrome P450 and chemical toxicology. *Chem. Res. Toxicol.* 21:70–83
32. Ames BN, Mcann J, Yamasaki E. 1975. Methods for detecting carcinogens and mutagens with the *Salmonella*/mammalian-microsome mutagenicity test. *Mutat. Res.* 31:347–64
33. Oda Y, Nakamura S, Oki I, Kato T, Shinagawa H. 1985. Evaluation of a new system (*umu*-test) for the detection of environmental mutagens and carcinogens. *Mutat. Res.* 147:212–29
34. Galloway SM, Aardema MJ, Ishidate M Jr, Ivett JL, Kirkland DJ, et al. 1994. Report from working group on in vitro tests for chromosomal abberations. *Mutat. Res.* 312:241–61
35. Sasaki YF, Sekihashi K, Izumiyama F, Nishidate E, Saga A, et al. 2000. The Comet assay with multiple mouse organs: comparison of Comet assay results and carcinogenicity with 208 chemicals selected from the IARC monographs and U.S. NTP Carcinogenicity Database. *Crit. Rev. Toxicol.* 30:629–799
36. Singh NP, McCoy MT, Tice RR, Schneider EL. 1998. A simple technique for quantitation of low levels of DNA damage in individual cells. *Exp. Cell. Res.* 175:184–91
37. Xhou X, Liberman RG, Skipper PL, Margolin Y, Tannenbaum SR, Dedon PC. 2005. Quantification of DNA strand breaks and abasic sites by oxime derivatization and accelerator mass spectrometry: application to γ-radiation and peroxynitrite. *Anal. Biochem.* 343:84–92
38. Kelly MC, White B, Smith MR. 2008. Separation of oxidatively damaged DNA nucleobases and nucleosides. Separation of oxidatively damaged DNA nucleobases and nucleosides on packed and monolith C18 columns by HPLC-UV-EC. *J. Chromatogr. B* 863:181–86
39. Sar DG, Montes-Bayon M, Ortiz LA, Blanco-Gonzalez E, Sierra LM, Sanz-Mendel A. 2008. In vivo detection of DNA adducts induced by cisplatin using capillary HPLC-ICP-MS and their correlation with genotoxic damage in *Drosophila melanogaster*. *Anal. Bioanal. Chem.* 390:37–44
40. Chowdhury G, Guengerich FP. 2009. Tandem mass spectrometry-based detection of C4′-oxidized abasic sites at specific positions in DNA fragments. *Chem. Res. Toxicol.* 22:1310–19
41. Chowdhury G, Guengerich FP. 2008. Direct detection and mapping of sites of base modification in DNA fragments by tandem mass spectrometry. *Angew. Chem. Int. Ed.* 47:381–84
42. Nomura Y, Fuchigami H, Kii H, Feng Z, Nakamura T, et al. 2006. Detection of oxidative stress–induced mitochondrial DNA damage using fluorescence correlation spectroscopy. *Anal. Biochem.* 350:196–201
43. Kondepati VR, Heise HM, Oszinda T, Mueller R, Keese M, et al. 2008. Detection of structural disorders in colorectal cancer DNA with Fourier-transform infrared spectroscopy. *Vib. Spectrosc.* 46:150–57
44. Kundu LM, Loppnow GR. 2007. Direct detection of 8-oxo-deoxyguanosine using UV resonance Raman spectroscopy. *Photochem. Photobiol.* 83:600–2
45. Collins A, Gedrick C, Vaughan N, Wood S, White A, et al. 2003. Measurement of oxidative DNA damage in human cells by chromatographic and enzymatic methods. *Free Radic. Biol. Med.* 34:1089–99
46. Mortelmans K, Zeiger E. 2000. The Ames *Salmonella*/microsome mutagenicity assay. *Mutat. Res.* 455:29–60
47. Iyer VN, Szybalski W. 1958. Two simple methods for the detection of chemical mutagens. *Appl. Microbiol.* 6:23–29
48. Ames BN, Whitfield HJ Jr. 1966. Frameshift mutagenesis in *Salmonella*. *Cold Spring Harb. Symp. Quant. Biol.* 23:221–25

49. Vignati L, Turlizzi E, Monaci S, de Grossi P, Kanter P, et al. 2005 An in vitro approach to detect metabolite toxicity due to CYP3A4-dependent bioactivation of xenobiotics. *Toxicology* 216:154–67
50. Gao J, Garulacan L, Storm S, Hefta S, Opiteck G, et al. 2004. Identification of in vitro protein biomarkers of idiosyncratic liver toxicity. *Toxicol. In Vitro* 18:533–41
51. Evans DC, Watt AP, Nicoll-Griffith DA, Baillie TA. 2004. Drug-protein adducts: an industry perspective on minimizing the potential for drug bioactivation in drug discovery and development. *Chem. Res. Toxicol.* 17:3–16
52. Park K, Williams DP, Naisbitt DJ, Kitteringham NR, Pirmohamed M. 2005. Investigation of toxic metabolites during drug development. *Toxicol. Appl. Pharm.* 207:S425–34
53. Kiskinis E, Suter W, Hartmann A. 2002. High throughput comet assay using 96-well plates. *Mutagenesis* 17:37–43
54. Flukiger-Isler S, Baumeister M, Braun K, Gervais V, Hasler-Nguyen N, et al. 2004. Assessment of the performance of the Ames II assay: a collaborative study with 19 coded compounds. *Mutat. Res.* 558:181–97
55. O'Brien P, Irwin W, Diaz D, Cofield H, Krejsa C, et al. 2006. High concordance of drug-induced human hepatotoxicity with in vitro cytotoxicity measured in a novel cell based model using high content screening. *Arch. Toxicol.* 80:580–604
56. Styles JA, Clark H, Festing MFW, Rew DA. 2001. Automation of mouse micronucleus genotoxicity assay by laser scanning cytometry. *Cytometry* 44:153–55
57. Shuga J, Zhang J, Samson LD, Lodish HF, Griffith LG. 2007. In vitro erthropoiesis from bone marrow–derived proginators provides a physiological assay for toxic and mutagenic compounds. *Proc. Natl. Acad. Sci. USA* 104:8737–42
58. Van Gompel J, Woestenborghs F, Beerens D, Mackie C, Cahill PA, et al. 2005. An assessment of the utility of the yeast GreenScreen assay in pharmaceutical screening. *Mutagenesis* 20:449–54
59. Hastwell PW, Chai LL, Roberts KJ, Webster TW, Harvey JS, et al. 2006. High specificity and high sensitivity genotoxicity assessment in a human cell line: validation of the GreenScreen HC GADD45α-GFP genotoxicity assay. *Mutat. Res.* 607:160–75
60. Benton MG, Glasser NR, Paleček SP. 2007. The utilization of a *Saccharomyces cerevisiae* HUG1P-GFP promoter-reporter construct for the selective detection of DNA damage. *Mutat. Res.* 633:21–34
61. Schwartz MP, Derfus AM, Alvarez SD, Bhatia SN, Sailor MJ. 2006. The smart petri dish: a nanostructured photonic crystal for real-time monitoring of living cells. *Langmuir* 22:7084–90
62. Zhu J, Wang X, Yu W, Abassi YA. 2006. Dynamic and label-free monitoring of natural killer cell cytoxtoxic activity using electronic cell sensor arrays. *J. Immunol. Methods* 309:25–33
63. Xing JZ, Zhu L, Jackson J, Gabos S, Sun XJ, et al. 2005. Dynamic monitoring of cytotoxicity on microelectrode sensors. *Chem. Res. Toxicol.* 18:154–61
64. Xiao C, Luong HT. 2005. Assessment of cytotoxicity by emerging impedance spectroscopy. *Toxicol. Appl. Pharmacol.* 206:102–12
65. Riley MR, Lucas P, Le Coq D, Juncker C, Boesewetter DE, et al. 2006. Lung cell fiber evanescent wave spectroscopic biosensing of inhalation health hazards. *Biotechnol. Bioeng.* 95:599–612
66. Kuang L, Biran I, Walt D. 2004. Living bacterial cell array for genotoxin monitoring. *Anal. Chem.* 76:2902–9
67. Mitchell R, Gu M. 2004. An *Escherichia coli* biosensor capable of detecting both genotoxic and oxidative damage. *Appl. Microbiol. Biotechnol.* 64:46–52
68. Mitchell R, Gu M. 2004. Construction and characterization of novel dual stress-responsive bacterial biosensors. *Biosens. Bioelectron.* 19:977–85
69. Lee J, Mitchell R, Kim B, Cullen D, Gu M. 2005. A cell array biosensor for environmental toxicity analysis. *Biosens. Bioelectron.* 21:500–507
70. Notingher I. 2007. Raman spectroscopy cell-based sensors. *Sensors* 7:1343–58
71. Buckmaster R, Asphahani F, Thein M, Xu J, Zhang M. 2009. Detection of drug induced cellular changes using confocal Raman spectroscopy on patterned single-cell biosensors. *Analyst* 134:1440–46
72. Mercey E, Obeid P, Glaise D, Calvo-Munoz ML, Guguen-Guillouzo C, et al. 2010. The application of 3D micropatterning of agarose substrate for cell culture and in situ comet assays. *Biomaterials* 31:3156–65
73. Lee M, Park C, Dordick J, Clark D. 2005. Metabolizing enzyme toxicology assay chip (MetaChip) for high throughput microscale toxicity analyses. *Proc. Natl. Acad. Sci. USA* 102:983–87

74. Lee M-Y, Kumar RA, Sukumaran SM, Hogg MG, Clark DS, et al. 2008. Three dimensional cellular microarray for high throughput toxicity analysis. *Proc. Natl. Acad. Sci. USA* 105:59–63
75. Fernandes TG, Diogo MM, Clark DS, Dordick JS, Cabral JMS. 2009. High-throughput cellular microarray platforms: applications in drug discovery, toxicology and stem cell research. *Trends Biotechnol.* 27:342–49
76. Wada KI, Taniguchi I, Kobayashi J, Yamato M, Okano T. 2008. Live cells–based cytotoxic sensorchip fabricated in a microfluidic system. *Biotechnol. Bioeng.* 99:1513–17
77. Dittrich PS, Manz A. 2006. Lab on a chip: microfluidics in drug discovery. *Nat. Rev. Drug Dev.* 5:210–18
78. Fojta M. 2005. Detecting DNA damage with electrodes. In *Electrochemistry of Nucleic Acids and Proteins*, ed. E Paleček, F Scheller, J Wang, pp. 386–482. Amsterdam: Elsevier
79. Paleček E. 2002. Past, present, and future of nucleic acids electrochemistry. *Talanta* 56:809–19
80. Kubicarova T, Fojta M, Vidic J, Havran L, Paleček E. 2000. Mercury film electrode as a sensor for the detection of DNA damage. *Electroanalysis* 12:1422–25
81. Cahova-Kucharkova K, Fojta M, Mozga T, Paleček E. 2005. Use of DNA repair enzymes in electrochemical detection of damage to DNA bases in vitro and in cells. *Anal. Chem.* 77:2920–27
82. Vacek J, Cahova K, Paleček E, Bullard DR, Lavesa-Curto M, et al. 2008. Label-free electrochemical monitoring of DNA ligase activity. *Anal. Chem.* 80:7609–13
83. Havran L, Vacek J, Cahova K, Fojta M. 2008. Sensitive voltammetric detection of DNA damage at carbon electrodes using DNA repair enzymes and an electroactive osmium marker. *Anal. Bioanal. Chem.* 391:1751–58
84. Zhang Y, Zhang H, Hu N. 2008. Using exonuclease III to enhance electrochemical detection of natural DNA damage in layered films. *Biosens. Bioelectron.* 23:1077–82
85. Hvastkovs EG, Buttry DA. 2010. Recent advances in electrochemical DNA hybridization sensors. *Analyst* 135:1817–29
86. Boal AK, Barton JK. 2005. Electrochemical detection of lesions in DNA. *Bioconj. Chem.* 16:312–21
87. Buzzeo MC, Barton JK. 2008. Redmond red as a redox probe for the DNA-mediated detection of abasic sites. *Bioconjug. Chem.* 19:2110–12
88. Wong ELS, Gooding JJ. 2007. The electrochemical monitoring of the perturbation of charge transfer through DNA by cisplatin. *J. Am. Chem. Soc.* 129:8950–51
89. Satterwhite JE, Pugh AM, Danell AS, Hvastkovs EG. 2011. Electrochemical detection of anti–benzo[*a*]pyrene diol epoxide DNA damage on *TP53* codon 273 oligomers. *Anal. Chem.* 83:3327–35
90. Rusling JF. 2004. Sensors for toxicity of chemicals and oxidative stress based on electrochemical catalytic DNA oxidation. *Biosens. Bioelectron.* 20:1022–28
91. Rusling JF. 2005. Sensors for genotoxicity and oxidized DNA. In *Electrochemistry of Nucleic Acids and Proteins*, ed. E Paleček, F Scheller, J Wang, pp. 433–50. Amsterdam: Elsevier
92. Lvov Y. 2001. Thin film nanofabrication by alternate adsorption of polyions, nanoparticles, and proteins. In *Handbook of Surfaces and Interfaces of Materials*, Vol. 3, ed. RW Nalwa, pp. 170–89. San Diego: Academic
93. Rusling JF, Hvastkovs EG, Hull DO, Schenkman JB. 2008. Biochemical applications of ultrathin films of enzymes, polyions and DNA. *Chem. Commun.* 2008:141–54
94. Zhou L, Yang J, Estavillo C, Stuart JD, Schenkman JB, et al. 2003. Toxicity screening by electrochemical detection of DNA damage by metabolites generated in situ in ultrathin DNA-enzyme films. *J. Am. Chem. Soc.* 125:1431–36
95. Johnston DH, Glasgow KC, Thorp HH. 1995. Electrochemical measurement of the solvent accessibility of nucleobases using electron transfer between DNA and metal complexes. *J. Am. Chem. Soc.* 117:8933–38
96. Yang J, Wang B, Rusling JF. 2005. Genotoxicity sensor response correlated with DNA nucleobase damage rates. *Mol. Biosyst.* 1:251–59
97. Miao W, Choi JP, Bard AJ. 2002. Electrogenerated chemiluminescence 69: the tris(2,2′-bipyridine)ruthenium(II), $[Ru(bpy)_3^{2+}]$/tri-*n*-propylamine (TPrA) system revisited—a new route involving $TPrA^{*+}$ cation radicals. *J. Am. Chem. Soc.* 124:14478–85
98. Xu X-H, Bard AJ. 1995. Immobilization and hybridization of DNA on an aluminum(III) alkanebisphosphonate thin film with electrogenerated chemiluminescent detection. *J. Am. Chem. Soc.* 117:2627–31

99. Leland JK, Powell MJ. 1990. Electrogenerated chemiluminescence: an oxidative-reduction type ECL reaction sequence using tripropyl amine. *J. Electrochem. Soc.* 137:3127–31
100. Blackburn GF, Shah HP, Kenten JH, Leland J, Kamin RA, et al. 1991. Electrochemiluminescence detection for development of immunoassays and DNA probe assays for clinical diagnostics. *Clin. Chem.* 37:1534–39
101. Dennany L, Forster RJ, Rusling JF. 2003. Simultaneous direct electrochemiluminescence and catalytic voltammetry detection of DNA in ultrathin films. *J. Am. Chem. Soc.* 125:5213–18
102. Mugweru A, Rusling JF. 2002. Square wave voltammetric detection of chemical DNA damage with catalytic poly(4-vinylpyridine)-Ru(bpy)$_2^{2+}$ films. *Anal. Chem.* 74:4044–49
103. So M, Hvastkovs EG, Schenkman JB, Rusling JF. 2007. Electrochemiluminescent/voltammetric toxicity screening sensor using enzyme-generated DNA damage. *Biosens. Bioelectron.* 23:492–98
104. Thorp HH. 2004. Electrocatalytic DNA oxidation. *Top. Curr. Chem.* 237:159–81
105. Dennany L, Hogan CF, Keyes TE, Forster RJ. 2006. Effect of surface immobilization on the electrochemiluminescence of ruthenium-containing metallopolymers. *Anal. Chem.* 78:1412–17
106. Hvastkovs EH, So M, Krishnan S, Bajrami B, Tarun T, et al. 2007. Electrochemiluminescent arrays for cytochrome P450–activated genotoxicity screening. DNA damage from benzo[*a*]pyrene metabolites. *Anal. Chem.* 79:1897–906
107. Bajrami B, Hvastkovs EG, Jensen G, Schenkman JB, Rusling JF. 2008. Enzyme-DNA biocolloids for DNA adduct and reactive metabolite detection by chromatography–mass spectrometry. *Anal. Chem.* 80:922–32
108. Krishnan S, Hvastkovs EG, Bajrami B, Choudhary D, Schenkman JB, Rusling JF. 2008. Synergistic metabolic toxicity screening using microsome/DNA electrochemiluminescent arrays and nanoreactors. *Anal. Chem.* 80:5279–85
109. Hecht SS. 2003. Tobacco carcinogens, their biomarkers and tobacco-induced cancer. *Nat. Rev. Cancer* 10:733–44
110. Marnett LJ, Burcham PC. 1993. Endogenous DNA adducts: potential and paradox. *Chem. Res. Toxicol.* 6:771–85
111. Gangl ET, Turesky RJ, Vouros P. 2001. Detection of in vivo formed DNA adducts at the part-per-billion level by capillary liquid chromatography/microelectrospray mass spectrometry. *Anal. Chem.* 73:2397–404
112. Zamenhof S, Arikawa S. 1966. Depurination and alkylation of DNAs of different base compositions. *Mol. Pharmacol.* 2:570–73
113. Tarun M, Rusling JF. 2006. Genotoxicity screening using biocatalyst-DNA films and capillary LC-MS/MS. *Anal. Chem.* 78:624–27
114. Tarun M, Rusling JF. 2005. Quantitative measurement of DNA adducts using neutral hydrolysis and LC-MS. Validation of genotoxicity sensors. *Anal. Chem.* 77:2056–62
115. Lvov Y, Caruso F. 2001. Biocolloids with ordered urease multilayer shells as enzymatic reactors. *Anal. Chem.* 73:4212–17
116. Krishnan S, Hvastkovs EG, Bajrami B, Schenkman JB, Rusling JF. 2009. Metabolic toxicity of 4-(methylnitrosamino)-1-(3-pyridyl)-1-butanone (NNK) evaluated using electrochemiluminescent arrays and human cyt P450s. *Mol. Biosyst.* 5:163–69
117. Bajrami B, Krishnan S, Rusling JF. 2008. Microsome biocolloids for rapid drug metabolism and inhibition assessment by LC-MS. *Drug Metab. Lett.* 2:158–62
118. Bajrami B, Zhao L, Schenkman JB, Rusling JF. 2009. Rapid LC-MS drug metabolite profiling using microsomal enzyme bioreactors in a parallel processing format. *Anal. Chem.* 81:9921–29
119. Zhao L, Schenkman JB, Rusling JF. 2010. High throughput metabolic toxicity screening using magnetic particle bioreactors and LC-MS/MS. *Anal. Chem.* 82:10172–78
120. Zhao L, Schenkman JB, Rusling JF. 2010. Screening for reactive metabolites using electro-optical arrays featuring human liver cytosol and microsomal enzyme sources and DNA. *Chem. Commun.* 2010:5386–88
121. Greave P, Goonetilleke R, Nunn G, Topham J, Orton T. 1993. Two-year carcinogenicity study of tamoxifen in Alderley-Park Wistar–derived rats. *Cancer Res.* 53:3919–24
122. White INH. 2003. Tamoxifen: Is it safe? Comparison of activation and detoxication mechanisms in rodents and in humans. *Curr. Drug Metab.* 4:223–39

123. Zhao L, Krishnan S, Zhang Y, Schenkman JB, Rusling JF. 2009. Differences in metabolite-mediated toxicity of tamoxifen in humans vs. rodents elucidated with DNA/microsome electro-optical arrays and nanoreactors. *Chem. Res. Toxicol.* 22:341–47
124. Boocock DJ, Maggs JL, Brown K, White INH, Park BK. 2000. Major inter-species differences in the rates of *O*-sulphonation and *O*-glucuronylation of α-hydroxytamoxifen in vitro: a metabolic disparity protecting human liver from the formation of tamoxifen-DNA adducts. *Carcinogenesis* 21:1851–58

Annual Review of
Analytical Chemistry

Volume 5, 2012

Contents